

## Chapter 5

# Physiological relevance of the changes in hemodynamics for circulating blood cells in Abdominal Aortic Aneurysms

### A. Introduction

It has been observed that 75% of AAAs with a maximum diameter of 4.5 cm develop an intraluminal thrombus (ILT). A few steady-flow studies have suggested that the build up of the thrombus may be associated with the altered hemodynamic patterns that arise inside the AAA when compared to the flow in a healthy abdominal aorta (Bluestein *et al.* 1996; Peattie *et al.* 1996).

In the previous two chapters, we have shown that the leading event caused by the formation of an aneurysm is the detachment of the flow from the wall around peak systole. The flow separation leads to the formation of recirculating regions along the walls and of a large vortex that traverses the aneurysm. Shear layers develop at the rear of the vortex leading to the presence of high shear stresses in the bulk of the flow. Excluding very long aspect-ratio aneurysms, the vortex impinges on the distal wall in the late systole, inducing high negative WSS and large gradients of WSS in the distal half of the aneurysm, while the proximal half is dominated by low and oscillating WSS. The

effects that these changes in the mechanical stimuli might have on the activation state of circulating blood cells have never been studied in abdominal aortic aneurysms.

As discussed in the introduction, hemodynamic forces have an important effect on the functions of platelets and leukocytes. The purpose of this study is to measure both the magnitude and duration of the shear stresses acting on blood cells circulating inside AAAs, and to characterize their changes as the AAA enlarges. Although several studies have reported on platelet–wall interaction in arterial anastomoses (Longest & Kleinstuever 2003), stenosis (Einav & Bleustein 2004) and mechanical heart valves (Bluestein, Rambod & Gharib 2000; Yin *et al.* 2004), to the best of our knowledge, this is the first study to systematically quantify the effects of the aneurysmal dilatation on the time history of shear stress acting on individual blood cells, residence time, platelet activation level and possible deposition along the wall.

Precise measurements of the velocity field have been conducted in models of AAA using Particle Image Velocimetry (PIV). The trajectories of blood cells have been calculated from the measured velocity fields using a Lagrangian approach. The evolution of the shear-stress history on platelets and of platelet activation parameters are presented in section 3. The physiological consequences on the mechanisms of thrombosis are discussed in section 4.

## **B. Material and methods**

**Cell trajectories and total stress time history.** A post-processing code was developed to calculate the trajectories of a few blood cells released at time  $t_0$  at the entrance of the aneurysm with a zero initial velocity. Markers, representing the individual cells, were tracked both spatially and temporally inside the aneurysm, in a Lagrangian manner. In each symmetric aneurysm, ten cells have been continuously released during

one cardiac cycle from ten equally spaced locations along the entrance radius of the aneurysm. In the non-symmetric models, twenty cells had to be introduced spread along the vessel diameter, since the flow is no longer symmetric. The shape of the cells has not been reproduced in this study.

At each time step, the location to which the cells have traveled is calculated based on the phase-average of the velocity field measurements obtained with the PIV system (see Chapter 2 for the method and Chapter 3 and 4 for the results). Although the symmetry of the flow was shown to break down briefly in the systolic deceleration in symmetric models (section 2.D.1), the use of the phase-averaged velocity fields, which does not include the weak transition to turbulence, should limit the loss of symmetry. Therefore, we assume presently that the three-dimensional effects are small enough to guarantee that most of the cells remain in the symmetry plane of the aneurysm. This assumption may be challenged inside non-symmetric aneurysm, where 3-D effects are stronger. However, conducting the particle tracking in the plane of symmetry of the model should still provide a good approximation of the residence time and cell shear stress history. The fact that the flow in the perpendicular plane remains almost symmetric with respect to the plane of symmetry (Chapter 4) supports this assumption.

In order to smooth out the large time lag (0.084 s) between two PIV measurements, the velocity profiles are interpolated linearly at 25 intermediate time steps. This method of interpolation reduces the maximum distance traveled between two time steps (distance < 0.6 mm). Although the linearly interpolated field is not the exact velocity field, it prevents the large discontinuities in the trajectories that form otherwise. At each step, the cell is localized with respect to the grid, by finding the four closest grid points. The velocity of the cell is computed by interpolating the phase-averaged velocities at the 4 grid points, each velocity being weighted by a weight function proportional to the distance of the point to the cell. The new location of the cell is then calculated with a

second order accuracy (leap-frog method), knowing the cell velocity and the time step. Every 15 steps, an Euler scheme of first order accuracy has been used in order to avoid the divergence of the solution into 2 distinct trajectories. If the new position is located behind the aneurysm wall boundary, the cell is projected onto the aneurysm wall. This method prevents the cells from being artificially trapped inside the large wall steps that result from the coarse measurement grid. The code ensures that the cells are convected parallel to the wall, without crossing the boundary. The calculation of the cell trajectory ceases when the cell has left the aneurysm distally. However, in the case of large dilatation ratios, it may happen that a few cells become lodged along the walls in areas of reduced convection. An upper time limit had therefore to be introduced, set at 8 cardiac cycles, which was found to be sufficient for all the cells remaining in circulation to exit the aneurysm. The total-stress history is calculated for each cell along its trajectory, based on the total stress fields obtained from the space- and time- interpolation of the velocity fields measured with the PIV technique (see Appendix B for the definition of the total stress).

**Cell activation parameter (CAP).** As mentioned in the introduction, the activation of blood cells depends on the cell stress time history and on the time the cells are exposed to the stress. It is therefore assumed that the cell activation parameter (CAP) is directly proportional to the total stress and exposure time. Similarly to Yin *et al.* (2004) and Einav & Bluestein (2004), we calculated the CAP as the integral over time of the local total stress  $\tau(t)$  acting on a particular cell

$$CAP = \frac{1}{\tau_{mean,H} \cdot L / \bar{U}} \int_{t_0}^{t_1} \tau(t') dt', \quad (5.1)$$

where  $t_1$  is the time the cells left the aneurysm. The stress integral is non-dimensionalized by the mean total stress measured in the healthy parent vessel,  $\tau_{mean,H}$ , multiplied by the mean convective time  $L/\bar{U}$ .

Furthermore, we considered the case where the shear effects on the cells are not purely cumulative as assumed previously. We calculated the CAP incorporating a relaxation time-scale  $\Sigma$ , after which activation processes decay exponentially

$$\frac{d(CAP)}{dt} = \tau - \frac{CAP}{\Sigma}, \quad (5.2)$$

the solution of which is

$$CAP = e^{-t/\Sigma} \int_{t_0}^{t_1} \tau(t') e^{t'/\Sigma} dt'. \quad (5.3)$$

The introduction of a relaxation time-scale is in agreement with the experiments, which show that the state of activation is suppressed, when the high stress stimulus is stopped.

In both cases, blood cells are initialized with a zero activation parameter. *In vivo*, activation could occur upstream of the aneurysm, but the current calculation concentrates on the sole effect of the presence of an aneurysm on the circulating cells.

**Near-wall residence time (NWRT).** Besides activation, bringing platelets and leukocytes in the vicinity to the wall is crucial for thrombosis to occur. This is one of the mechanisms through which convective flow patterns may greatly affect thrombosis. To quantify this effect, we measured the near-wall residence time (NWRT), first introduced by Longest & Kleinstreuer (2003). It is the integral of the average residence time weighted by the square of the distance,  $h$ , of the blood cell to the wall, calculated along the trajectory of each cell:

$$NWRT = \frac{\bar{U}L}{T} \int_{t_0}^{t_1} \frac{1}{h^2} \left( \frac{\Delta x^2 + \Delta y^2}{u^2 + v^2} \right)^{1/2} dt', \quad (5.4)$$

where  $\Delta x$  and  $\Delta y$  are the distances traveled in the  $x$ - and  $y$ -directions in between two time steps. The time- and space- averaged characteristic velocity in the parent vessel  $\bar{U}$  has been incorporated with the length of the aneurysm  $L$  and the period  $T$  to non-dimensionalize the residence time.

## C. Results

### 1. Influence of the AAA on the cell trajectories, residence time and stress history

The trajectories of ten blood cells have been calculated in all the models indicated in Table 5.I, when released at the ten different instants of times that compose one cardiac cycle. Figure 5.1 (a) shows the trajectories of the cells in the case of a medium dilatation ratio  $D/d = 2.1$  (model 5). The cells have been released at  $y/d = -0.8$  at time C. The cells are first confined inside the large jet that discharges into the aneurysm. But in the diastole, as their velocity decreases, they are entrained into the vortex structures and recirculating flow regions. Most of the cells recirculate in the distal half of the aneurysm, remaining in the region where most of the vortex structures are present.

One common pattern is the convection of cells towards the wall. As the cells recirculate, they are periodically led to travel very close to the wall. The time history of total stress experienced by these cells is plotted in Figure 5.1 (b). One can notice that all the cells experience highly fluctuating stresses, with high peak values occurring when the cells are present close to the wall at peak systole. Some of the cells exit the vortical flow after one cardiac cycle, while others stay for longer periods of time (up to five cardiac cycles, in this particular case). This entrainment of the cells into the vortical structures and recirculating flow regions persists throughout the cycle. Very few cells travel inside the aneurysm without being disturbed by its presence.

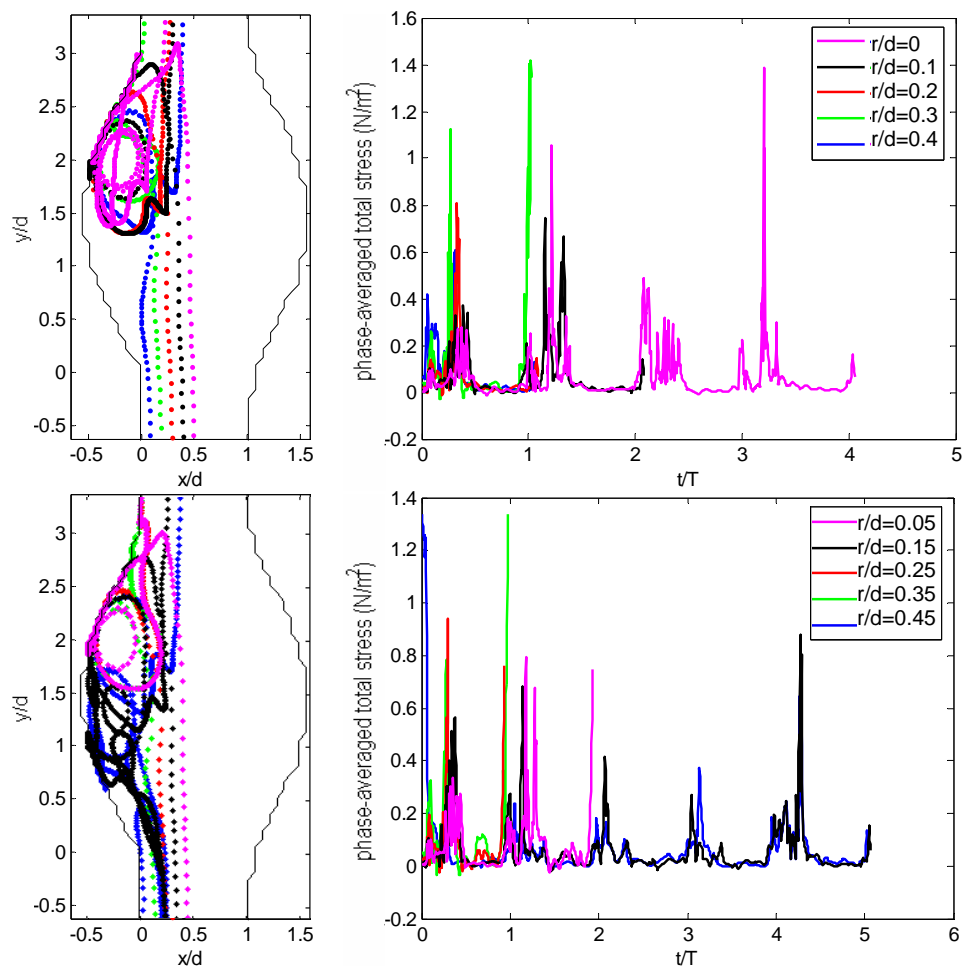


Figure 5.1: Trajectories and stress history for the 10 cells released in model 5 ( $D/d = 2.1$ ,  $L/d = 2.9$ ) at  $y/d = -0.8$  at time  $C$ .

Abdominal aortic aneurysms therefore have a very strong effect on the trajectories and stress history on blood cells. The flow in the healthy aorta has been detailed in Chapter 3. From the velocity profiles, shown in Figure 5.2 (a), one can deduce that the trajectories of the cells are rectilinear ( $u = 0$ ) and that a large number of cells experience minimal stress stimulation during their transit. The blunt velocity profiles give rise to a zero-stress condition in the bulk of the vessel throughout the cardiac cycle (Figure 5.2 (b)). Contrary to the case observed in an aneurysm, only the cells confined between the wall ( $y/d = 0$ ) and  $y/d \sim 0.2$  are exposed to some level of stress in a healthy vessel. The typical residence time of a cell inside an aneurysm of length  $L$  is  $L/\bar{U}$ . In the case of

model 5 ( $D/d = 2.1$ ), characterized by an aspect ratio of  $L/d = 2.9$ ,  $L/\bar{U} = 0.45T$  when the actual average residence time is  $3.44T$ . This shows that the presence of the aneurysm largely increases the residence time. The average stress the cells are subjected to across the vessel also increases in the aneurysm, the average stress being 63% higher than in the healthy vessel.

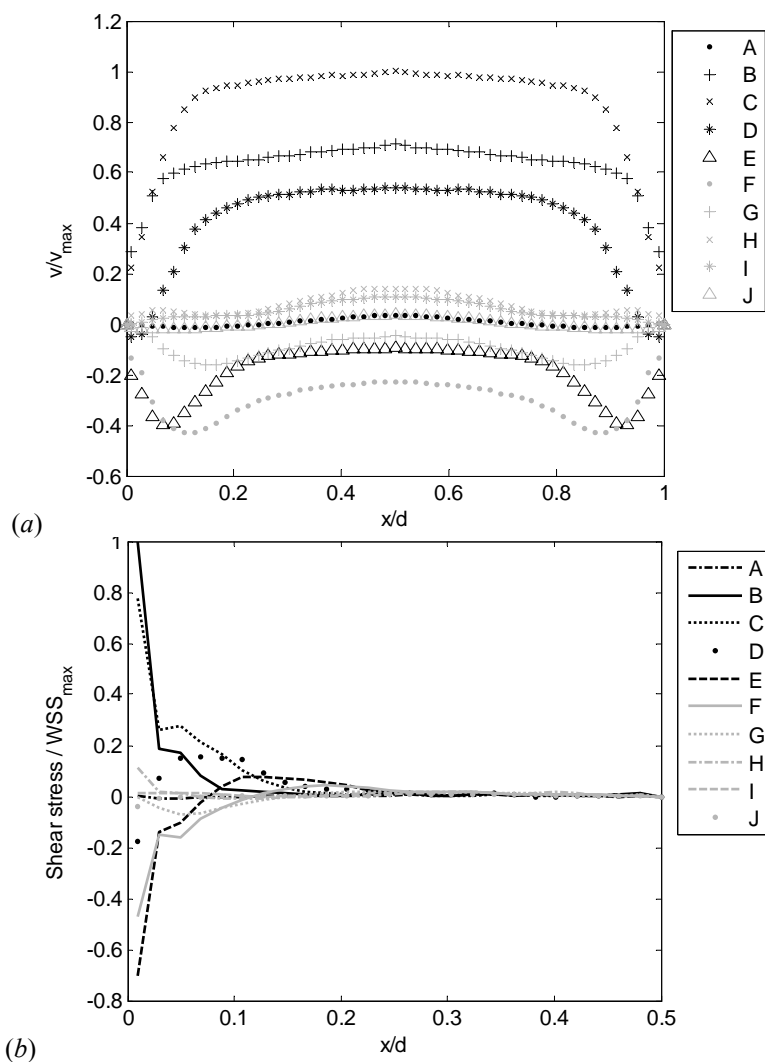


Figure 5.2: (a) Velocity and (b) stress profiles across a healthy vessel at the 10 instants of time that compose one cardiac cycle. The stress profiles are only shown for half the vessel.

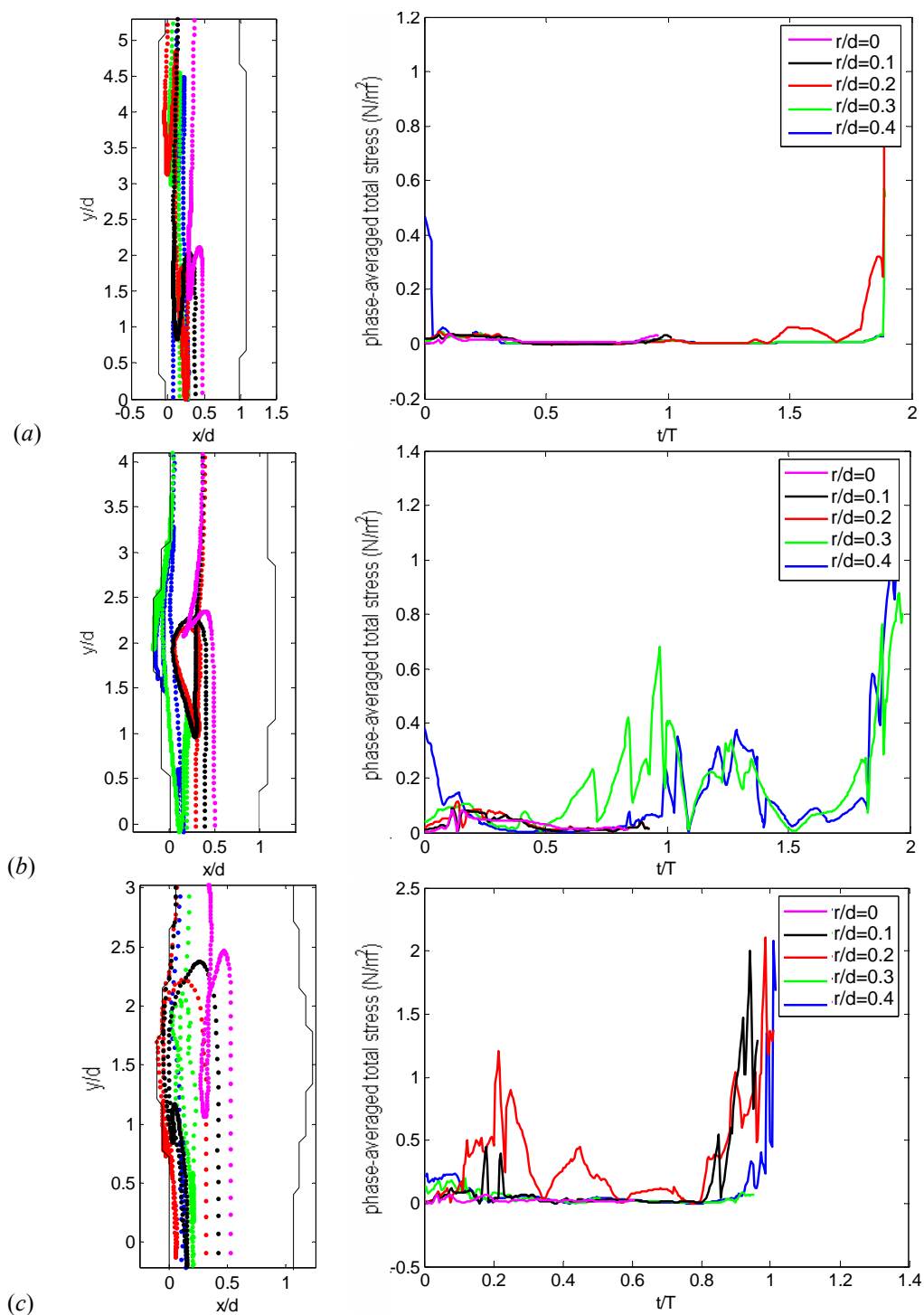


Figure 5.3: Effect of the decrease in the aspect ratio on the trajectories and stress history of cells. The cells were respectively released in model 11 –  $L/d = 5.2$  (a), model 6 –  $L/d = 3.9$  (b) and model 1 –  $L/d = 2.9$  (c) during systole (time C) at  $y/d = -0.8$ .

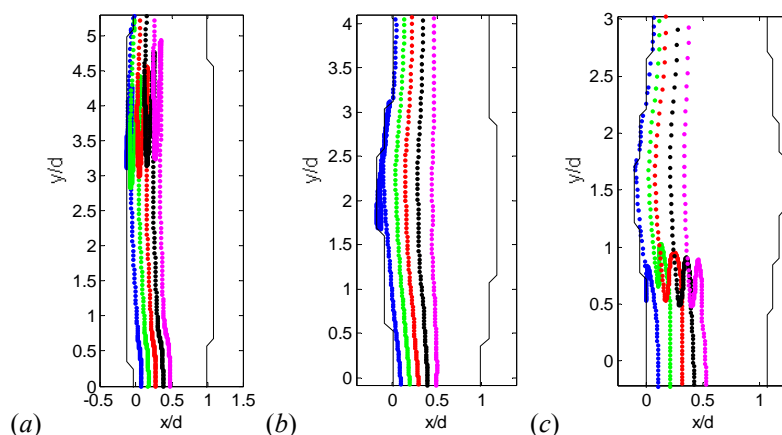


Figure 5.4: Trajectories of cells released in model 11 –  $L/d = 5.2$  (a), model 6 –  $L/d = 3.9$  (b) and model 1 –  $L/d = 2.9$  (c) during diastole (time G) at  $y/d = -0.8$ .

## 2. Effects of the aspect ratio

The velocity measurements have shown that the wall shear stresses depend on the geometric parameters of the aneurysm,  $L/d$ ,  $D/d$  and  $\beta$ . We report here how the blood cells are conjointly affected by the enlargement of the aneurysm. It was chosen to show the effects of the aspect ratio ( $L/d$ ) in incipient aneurysms, in order to gain some insight on the possible mechanisms responsible for the formation of AAAs. The three models, models 11, 6 and 1, have the same dilatation ratio ( $D/d = 1.3$ ), which is below the critical ratio of 1.5 used clinically to define an AAA. The length of the models has been decreased from an aspect ratio of 5.2 to 3.9 and finally 2.9. The pathlines and stress history are shown in Figure 5.3 for five cells introduced after the peak systole (time C). In the model with the largest aspect ratio (model 11), only the cells released at time C experience the effects of the very weak vortex shed between time C and D from the proximal neck. The trajectories are slightly skewed towards the centerline, when they follow the aneurysm shape at any other time (see Figure 5.4 (a)). However, the mean stress averaged over all the cells remains identical to the healthy vessel case. As the aspect ratio decreases, the vortex ring strengthens and a recirculating zone is formed.

Thus, the mechanism of active transport of the cells towards the wall already takes place at dilatation ratios as small as 1.3 and aspect ratios smaller than 4.

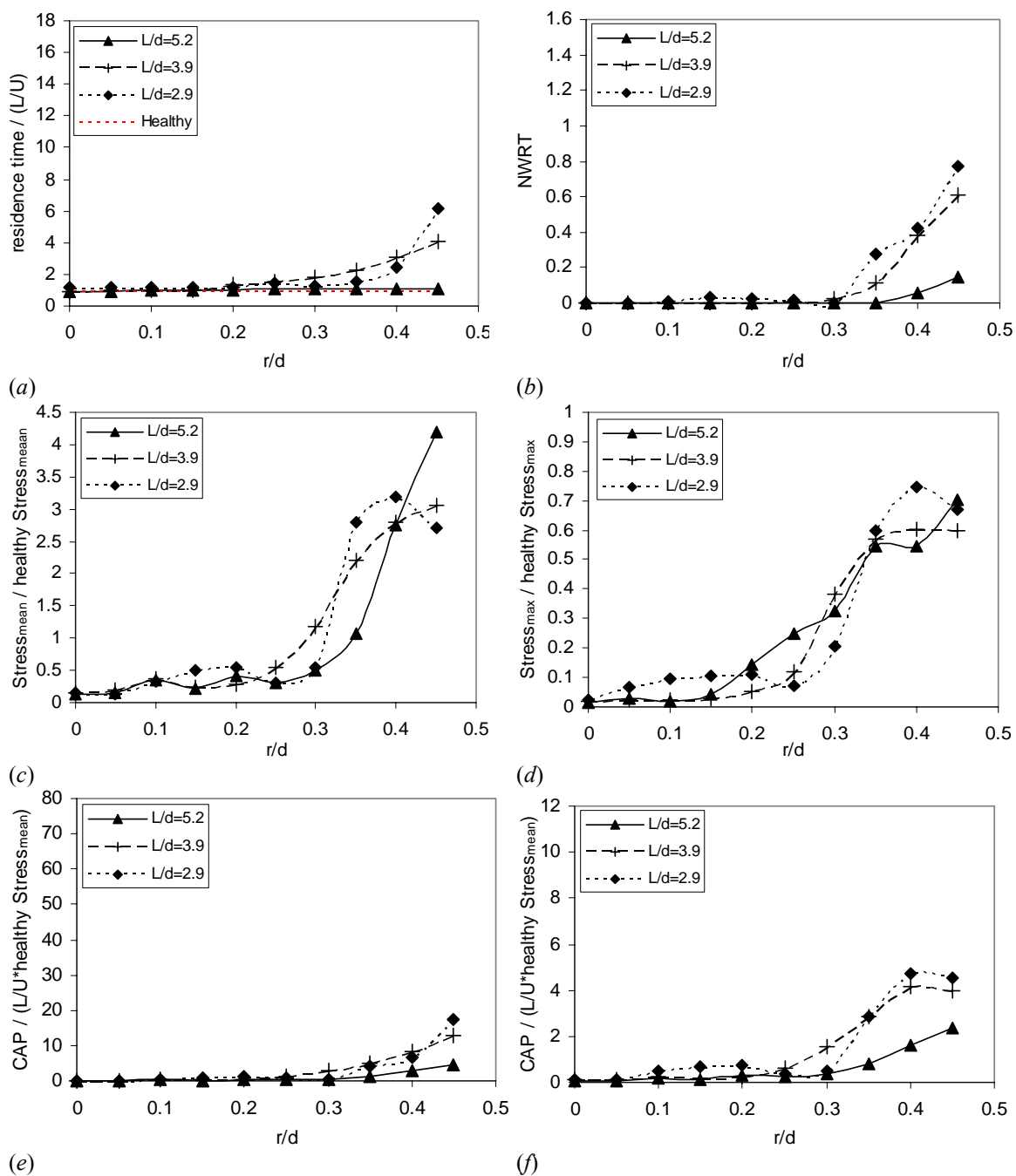


Figure 5.5: Comparison of the residence time (a), near wall residence time (b), mean (c) and peak (d) values of the stress and platelet activation parameters with (e) and without (f) the input of a relaxation time in models with decreasing aspect ratio. The dilatation ratio and asymmetry parameter are kept constant.  $r/d$  indicates the location where the

cells have been released in the parent vessel. The calculated quantities represent the averaged value over all the cells released at a specific location at 10 instants of time in one cardiac cycle.

Figure 5.5 compares the time-averages of the different parameters introduced in section B, when decreasing the aspect ratio: the residence time non-dimensionalized by the typical residence time in a healthy vessel ( $L/\bar{U}$ ), the near wall residence time (NWRT), the mean/peak stress non-dimensionalized by the corresponding value in the healthy vessel and finally the cell activation parameter (CAP) calculated with and without a relaxation time. There is a consistent increase of all these parameters when the aspect ratio of the aneurysm is decreased. One can also observe that all these parameters decrease as the position of cell release gets further from the wall. Similarly to a healthy aorta, it is the cells closest to the wall that experience longer residence time and higher stress values, which results in a higher cell activation parameter for these cells. The cells located between  $r/d = 0$  and 0.3 experience almost identical residence times ( $\sim L/\bar{U}$ ) and stress as in the healthy vessel. Still, a small increase in the residence time is noticeable in the model with the smallest aspect ratio (model 1), in which the blood cells from the center of the vessel start to be entrained in the incipient recirculating flow regions.

### 3. Effect of the dilatation ratio

The dilatation ratio has been linearly increased from 1.3 to 2.1 to study the effects that the aneurismal enlargement might have on the cells. The results are shown in models 1 to 5 that are characterized by the smallest aspect ratio ( $L/d = 2.9$ ), since increasing the aspect ratio has been shown to attenuate the effects of the dilatation parameter. The trajectory and stress time history of a few cells introduced at time C for  $D/d = 1.5$  (model 2) and  $D/d = 1.9$  (model 4) are shown in Figure 5.6. They can be considered in conjuncture to Figures 5.1 and 5.3 (c), which show the results for  $D/d = 2.1$  (model 5)

and  $D/d = 1.3$  (model 1) respectively. The size and strength of the vortex ring increases as  $D/d$  increases, which leads to a larger recirculating region. The likelihood for the cells to be entrained into the recirculating region therefore increases with the dilatation ratio. As  $D/d$  increases, more cells might be enclosed in a slow transitional motion along the vessel wall, in which cells remain for long residence times (longer than eight time the healthy residence time) as observed in Figure 5.6 for the cells introduced at  $y/d = 0.1$ . This phenomenon of rampant motion along the wall leads to an increase in the near wall residence time.

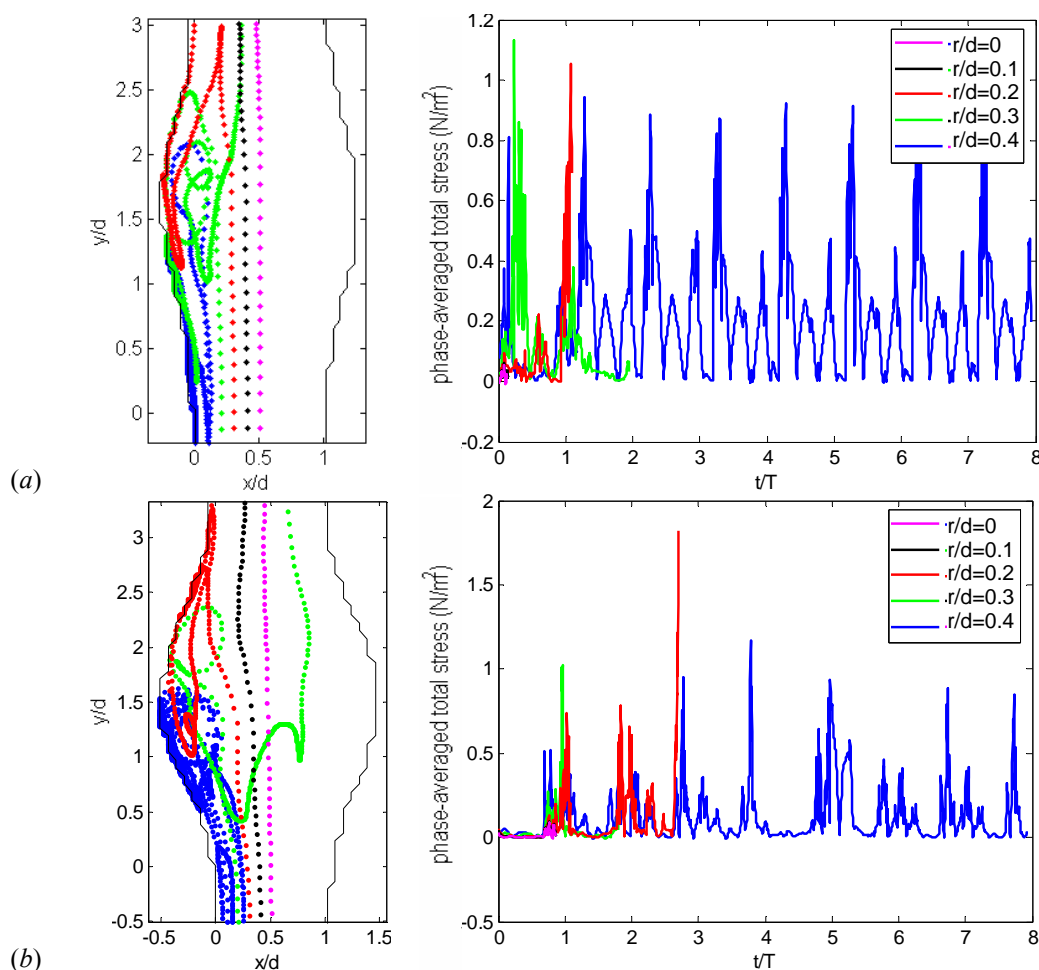


Figure 5.6: Trajectories and stress history of cells released in models 2 –  $D/d = 1.5$  (a) and model 4 –  $D/d = 1.9$  (b) during systole (time C) at  $y/d = -0.8$ .

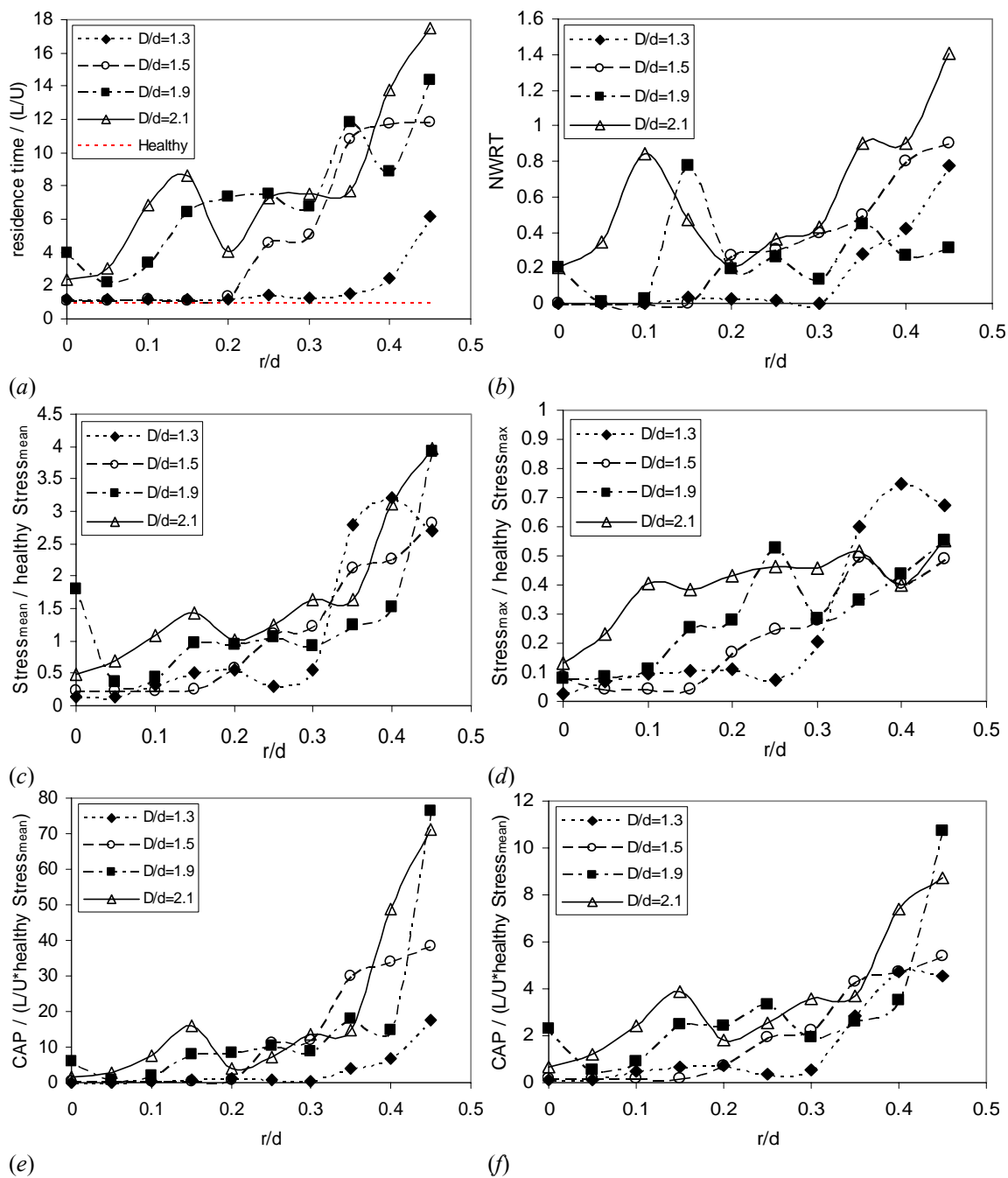


Figure 5.7: Comparison of the residence time (a), near wall residence time (b), mean (c) and peak (d) values of the stress and platelet activation parameters with (e) and without (f) the input of a relaxation time, when increasing the dilatation ratio. The aspect ratio and asymmetry parameter are kept constant.  $r/d$  indicates the location where the cells have been released in the parent vessel. The calculated quantities represent the averaged value over all the cells released at a specific location at 10 instants of time in one cardiac cycle.

The evolution of the cell activation parameters are plotted in Figure 5.7. As far as the cell response are concerned, one can make a clear cut at  $D/d = 1.5$ . Up to this aneurysm size (models 1 and 2), the cells in the bulk of the aneurysm maintain a normal residence time and low stress exposure, similar to the values in a healthy vessel. However, when the dilatation ratio exceeds 1.5, the residence times and mean and total stresses markedly increase for all the cells regardless of their position across the vessel. The activation parameter therefore increases to a non-zero value throughout the vessel, all the cells being susceptible to activate.

#### 4. Effects of the asymmetry parameter

As we have seen in Chapter 4, mid-size aneurysms tend to further grow non-symmetrically. The effect of the increase in the model asymmetry was therefore studied in larger size aneurysms, although the maximum diameter was kept under the critical size of 4.5 cm, above which an intraluminal thrombus is more likely to form. The trajectories and stress history are represented in Figure 5.8 inside models 17 (*a*) and 18 (*b*), which are respectively characterized by an asymmetry parameter of 0.5 and 1.

The cells are first convected towards the posterior wall, their trajectories being influenced by the shedding of a strong vortex from the proximal anterior wall. The vortex then impinges on the posterior wall entraining the cells into the recirculating region, where they remain for a few cardiac cycles. The calculation of the cells' pathlines shows how the recirculating region extends over the entire aneurismal cavity in the case of non-symmetric aneurysms. Surprisingly, the residence time is found to decrease as the asymmetry parameter is increased. In the model of medium eccentricity ( $\beta = 0.5$ ), the vortical flow structure traps cells for residence times 30% higher than in the model of maximum eccentricity ( $\beta = 1$ ) (Figure 5.9 (*a*)). Contrary to the symmetric models, the residence times, stress intensity and activation parameter no longer depend on  $r/d$  (Figure

5.9). The large recirculation induces a very strong mixing inside the aneurysm, which suppresses the radial dependency. Although no cell experiences the very high values of the parameters measured in symmetric aneurysms for cells introduced close to the wall, all the parameters maintain much higher values than in a healthy vessel, the mean stress being for example 40% higher.

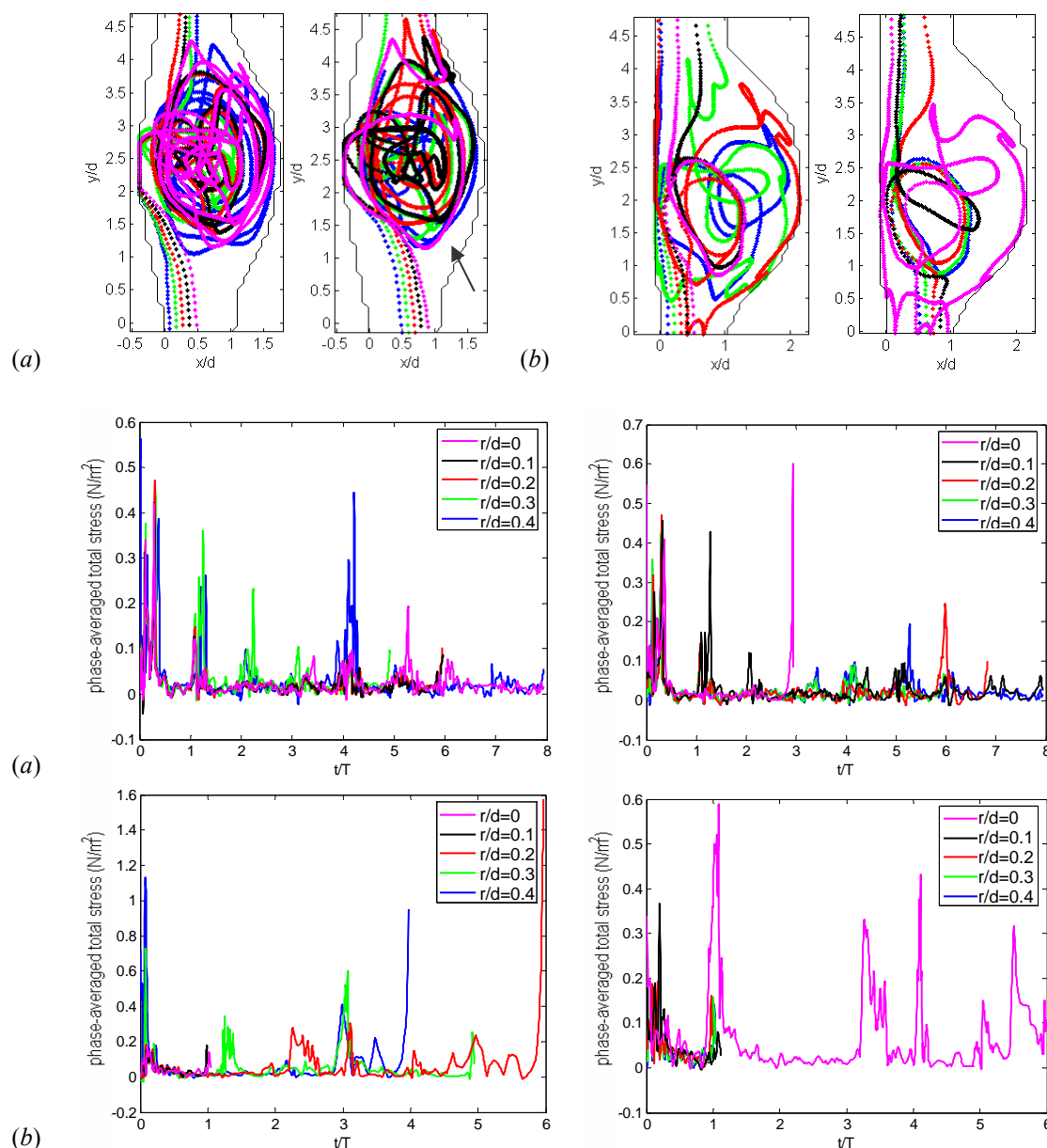


Figure 5.8: Trajectories and stress history of cells released in models 17 –  $\beta = 0.5$  (a) and 18 –  $\beta = 1$  (b) during systole (time C) at  $y/d = -0.8$ .

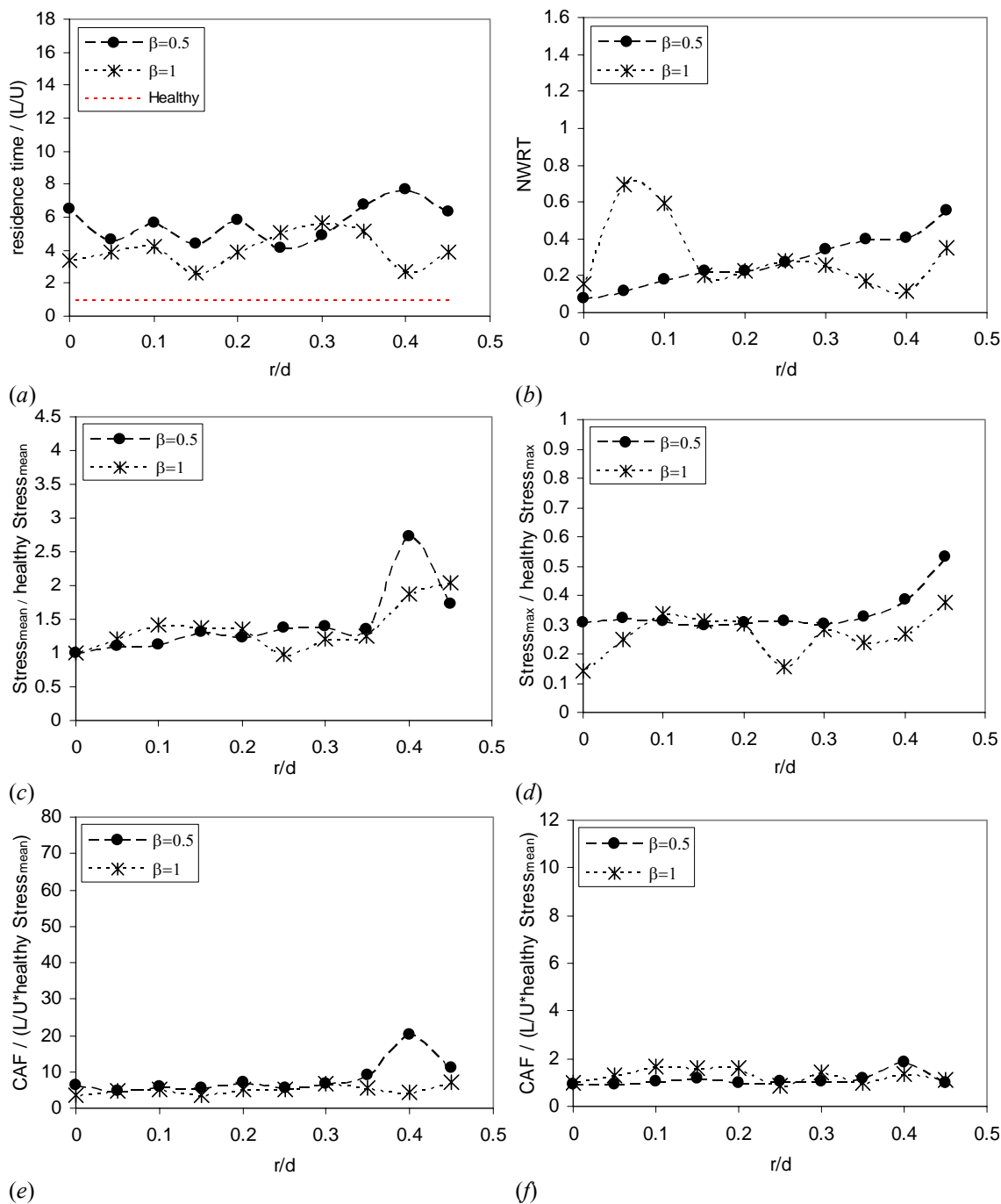


Figure 5.9: Comparison of the residence time (a), near wall residence time (b), mean (c) and peak (d) values of the stress and platelet activation parameters with (e) and without (f) the input of a relaxation time when increasing the asymmetry parameter.  $r/d$  indicates the location where the cells have been released in the parent vessel. The calculated quantities represent the averaged value over all the cells released at a specific location at 10 instants of time in one cardiac cycle.

## D. Discussion

The purpose of this study is to analyze the mechanisms that might account for the formation of an intraluminal thrombus. The important question to be elucidated is the role that the “disturbed” flow and stress conditions might play on the thrombus formation in AAAs. In order to measure how blood cells are affected by the growth of the aneurysm, a code has been developed to follow blood cells inside the aneurysm in a Lagrangian way and quantify their individual residence time and time history of stress. The cells’ trajectories are calculated using the PIV measurements of the velocity field, interpolated both in space and time. Special care has been taken to compute appropriately the transport close to the wall.

As the AAA enlarges, the platelets, leukocytes and red blood cells are locally subjected to higher levels of shear stresses. High shear stresses are formed inside the aneurysm as a result of the flow separation and formation of a large vortex. They occur inside the internal shear layers and to a larger extent at the walls, at the points of impact of the vortices. The peculiarity of the aneurismal flow topology is to transport the cells towards the wall, right into these regions of higher shear stresses. In these regions, the cells may become moderately activated, which may lead to a weak aggregation of the cells to one another. It has been shown by Wurzinger et al. (1985) that only such an active transport of the cells towards the wall can lead to the adhesion of activated platelet to the walls and to their aggregation. But without any further stimulation, the aggregates are known to dissolve very quickly. The moderate state of activation and aggregation can however be reinforced by the entrainment of the cells into regions of low stresses. When the translational motion of the cells is hindered by the presence of the wall, the cells are forced into the recirculating flow region, being entrained by the nearby vortex. The cells thus enter a region of very low shear stresses, which is known to foster aggregation (Alveriadou *et al.* 1993). The crucial parameter is the time the cells remain inside the

recirculating regions. Based on steady-flow experiments, Huang & Hellum (1993) have found that residence time of the order of at least 10 s is required for significant shear-induced aggregation. Although the pulsatile nature of the flow might influence their conclusion, our results show that such long residence times occur inside the aneurysm, if large enough. Moreover, we showed that, when recirculating, the cells are periodically exposed to higher stresses, since they are regularly brought in contact with the walls. This alternate high/very low stress stimulation along with long residence times might be responsible for cell activation and the convective patterns might then foster deposition along the wall.

All these phenomena are strongly dependent on the size of the aneurysm. Since the mechanisms for cell activation and aggregation depend on the presence of a strong vortex, regions of high wall shear stresses and moderately large regions of slowly recirculating flow, they may only occur in developed aneurysms. The calculation of the different activation parameters has shown the build-up of activation processes as the aneurysm grows. The time- and space-averaged values of all these parameters are represented in Figure 5.10. Figure 5.10 (a) indicates that decreasing the aneurysm aspect ratio may increase the residence time by a factor of 2, when the increase in dilatation ratio may lead to a 4.2-fold increase in both the residence time and near-wall residence time (Figure 5.10 (b)). The dilatation ratio influences similarly the mean value of the stresses acting on the cells and cell activation parameter (Figure 5.10 (c-e)), giving rise to a 20-fold increase of the CAP in the case of a medium-size aneurysm ( $D/d = 2.1$ ) as compared to a healthy vessel. Figures 5.10 (e) and (f) show that, although more physical, incorporating a relaxation time in the calculation of the cell activation parameter provides similar results to the simple integration of the stress simulation over time.

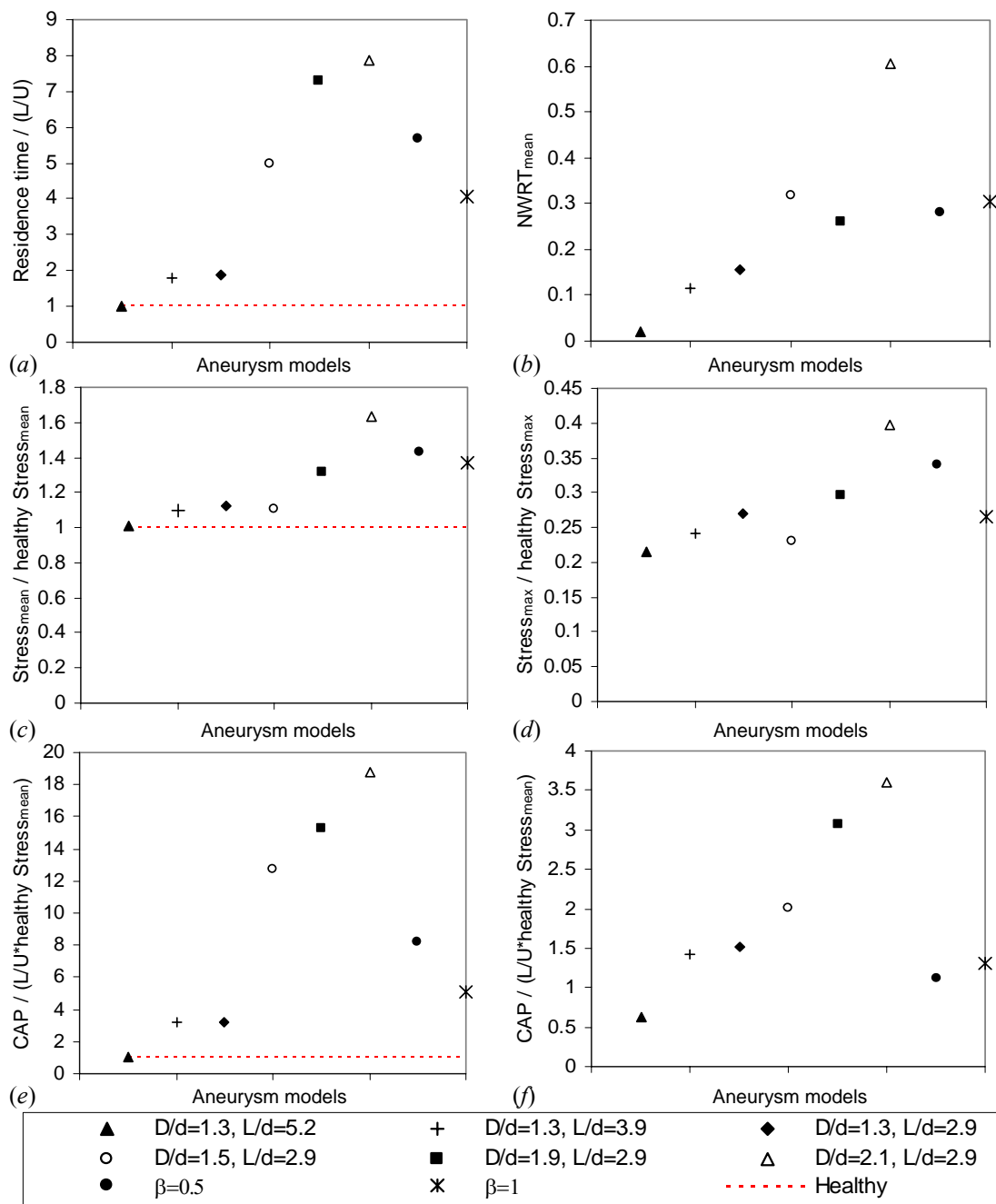


Figure 5.10: Effects of respectively the aspect ratio, dilatation ratio and asymmetry parameter on the mean values of the residence time, near wall residence time, mean and peak values of the stress and platelet activation parameters with or without the input of a relaxation time. These quantities, time- and space-averaged over all the cells released inside the models, are plotted for each model (abscissa).

An important phenomenon is the increase in the number of blood cells enclosed in the recirculating zone as the aneurysm grows. Small size aneurysms preserve an intact bulk region. But as the aneurysm reaches larger sizes, all the cells become likely to be exposed to the alternate pattern of high/low stresses for long residence times. Moreover, the persistence of the cell recirculation inside the aneurysm throughout the cardiac cycle only occurs when  $D/d > 1.9$ . In small size aneurysm, the recirculating structures are rapidly broken down in the diastole, when they persist in larger size aneurysms. These structures are the strongest in the non-symmetric models, especially in medium eccentricity models ( $\beta \sim 0.5$ ). The recirculating zone takes over the whole aneurysmal cavity, where cells move steadily at low velocities.

The activation and aggregation states of circulating cells are also highly affected by the activation state of the endothelial cells. The endothelial cells lining the vessels react to the changes in mechanical stimuli in the AAA. They have been shown to get activated both in regions of large gradients of wall shear stresses (as in the distal half of the AAA) (DePaolo et al. 1992; Tardy *et al.* 1997; Nagel *et al.* 1999) and in regions of low and oscillating wall shear stresses (as in the proximal half of the AAA) (Helmlinger, Berk & Nerem 1995; Moore *et al.* 1994). The cell tracking showed that the blood cells preferentially come very close to the wall in these 2 distinct regions: the cells are transported into the distal wall and then entrained upstream into the recirculating zone. The activated state of the endothelial cells fosters wall adhesion of the already partially aggregated blood cells and the release of chemical signals that potentiate the activation of platelets and leukocytes. Inflammation of the endothelium will therefore provide the optimal cell-adhesive conditions that may contribute to the pathogenesis of an intraluminal thrombus.

The thrombus is likely to develop in the detached flow region (Reininger *et al.* 1995) until the endoluminal channel is of the same diameter as the parent vessel. The infrarenal

abdominal thrombus is the only case of a thrombus that does not occlude the entire cavity and through which flow is maintained. The thrombus may provide some support to the weakened wall. However, this gain in structural strength is at the cost of a drastic reduction in oxygen diffusion to the medial layer, the disappearance of all endothelium-derived regulatory processes and the onset of inflammatory-mediated degenerative conditions throughout the arterial wall and within the thrombus itself. All these factors are known to contribute to the further deterioration of the medial layer, which is key to the structural strength of the wall and to the continued or even accelerated enlargement of the AAA (Kazi *et al.* 2003).

## **E. Conclusion**

In this study, we have shown that cell activation processes are likely to occur inside abdominal aortic aneurysms and that they may account for the formation of an intraluminal thrombus inside the aneurysm. A post-processing code was developed to track individual blood cells both spatially and temporally using the PIV measurements of the velocity and stress field inside the aneurysm. In order to quantify the levels of cell activation, we have calculated the trajectories of circulating cell as well as the magnitude and duration of the stresses acting on them. The effects of the aneurysm enlargement have been considered by changing systematically the geometric parameters of the models.

The parametric study shows that cell activation may be the result of the formation of regions of larger shear stresses in the internal shear layers and along the walls, at the locations of impact of the vortices. High shear stresses may activate cells and lead to their weak aggregation. The size and strength of the vortices have been shown to increase as the aneurysm grows, which accounts for the increase in the mean shear stresses acting on the cells (up to 60% higher in a medium size aneurysm) and in the number of cells being

entrained into the recirculating regions. As the aneurysm grows in size, a larger number of cells are subjected to low stress conditions, recirculating at low speed for several cardiac cycles. These cells are periodically subjected to higher shear stresses when brought in the vicinity of the wall at peak systole. Furthermore, as the dilatation ratio increases, the separated flow regions become larger in size, which leads to an increase in the cell residence times. An 8-fold increase of the residence time has been measured in a medium size symmetric aneurysm. On the contrary, increasing the aspect ratio reduces the pathological effects induced by the aneurismal dilatation.

From the results of this study, we hypothesize that the transition towards a non-axisymmetric shape is necessary for an intraluminal thrombus to form. In symmetric aneurysms, the flow reattaches to the walls at every systolic push, so that patterns of constantly recirculating cells hardly arise. The amount of cell deposition along the walls is also likely to be considerably reduced, since cell aggregates may be entrained from the wall at every cycle. In the case of non-symmetric aneurysms, however, all the thrombotic flow conditions are met. The blood cells have been shown to recirculate into the aneurysm cavity in a quasi-steady slow circular motion for long residence times. Since flow reattachment does not occur for large asymmetry parameters, a thrombus may form along the anterior wall, in regions such as the one indicated by an arrow on Figure 5.8 (a). Furthermore, inflammation processes are very likely to occur in the anterior wall, since the endothelial cells are subjected to almost zero wall shear stresses. Quasi-static flow conditions are known to activate the endothelial cells and possibly lead to their apoptosis and later exposure of submatrix collagen. They also lead to the increase of the wall porosity, possibly resulting in cholesterol deposit inside the walls. These injured and inflamed wall regions send signals to recruit platelets and leukocytes, which fosters thrombus formation.

This study was the first one to analyze possible cell activation processes inside AAAs. The changes in the mechanical stimuli acting on the cells and in their residence time have been quantified during the aneurysm enlargement. The results of this study could help choose physiologically relevant patterns of shear stresses and residence times for new studies on circulating cells under pulsatile flow conditions. These studies would provide the much-needed information that would validate or invalidate our postulates.

## **Chapter 6**

### **General conclusion and perspectives**

#### **A. General conclusion**

For the last few decades, it has been recognized that abdominal aortic aneurysms result from a complex interplay between mechanical stimuli and biochemical reactions occurring inside the arterial wall. Hemodynamic stresses (pressure and wall shear stresses) are thought to affect the mechanisms responsible for the formation, growth and rupture of AAAs, via their effects on the endothelial cells, smooth muscle cells and blood cells. Endothelial and smooth muscle cells act as sensors of the hemodynamic forces and actuators, transducing the signals into vasomotor responses. Experiments have shown that the cells react not only to the magnitude of the shear stresses, but also to their spatial and temporal variations. Perturbations from the baseline stress conditions alter the mechanisms of mechanotransduction for both types of cells. Circulating blood cells also respond to the fluid stresses and may become activated in case of exposure to high or very low stresses. The main objective of the dissertation was to characterize the changes in the hemodynamic forces resulting from the enlargement of the abdominal aorta, in order to provide some insights on the role that the hemodynamic forces play in the

etiology and progression of the disease. We have measured the spatial and temporal distribution of internal and wall shear stresses in idealized models of AAAs, using Particle Image Velocimetry. The use of a well-controlled geometry for the models enabled us to quantify systematically the effects that an increase in aneurysm diameter, length or asymmetry might have on the stress field, which would not have been possible in physiologically-correct models.

We have shown that, even in the case of dilatation ratios as small as  $D/d = 1.3$  (for  $L/d < 4$ ), the flow separates from the wall after the peak systole, which leads to the formation of a vortex structure and of a separated flow region along the walls. These changes in the flow topology modify the hemodynamic forces acting on the endothelial cells and on circulating blood cells, since distinct regions of higher shear stresses (in the shear layer and point of vortex impingement), very low shear stresses (in the separated zone) and large spatial and temporal gradients of shear stresses (around the point of flow reattachment) form inside the aneurysm. The study of very incipient aneurysms proved that even a small change in the vessel geometry drastically changes the flow structures and stresses. An abdominal aortic aneurysm may therefore be initiated by a change in the vessel morphology, such as an increased bending or contraction, known to cause flow separation. We can hypothesize that a healthy wall would readjust its shape to avoid the presence of flow separation, but the changes in the wall properties due to aging, hypertension or any other risk factor discussed in the introduction might prevent the natural healing processes.

We have found that most of the flow patterns that form in symmetric aneurysms persist in non-symmetric AAAs. Up to very large dilatation ratios, the flow remains attached to the walls in the systolic acceleration. This engenders a decrease in the WSS inside the aneurysm and therefore large GWSS at both necks. The flow only detaches from the proximal neck during the systolic deceleration. In the case of symmetric

aneurysms, a large start-up vortex ring forms and, as it propagates through the aneurysm, secondary vortex rings develop in the associated internal shear layers. When non-symmetric, the geometric configuration prevents the formation of a closed vortex ring and the strongest vortex is shed from the proximal anterior wall. The vortex structure has the shape of a hairpin. In the case of moderate aspect ratios, the shed vortices impinge on the opposite (section of the) wall, causing locally large WSS. Large gradients of WSS consequently form along the vessel wall, since, outside the small area affected by the vortex, the wall is exposed to very low and oscillating wall shear stresses. During the diastole, the flow reversal causes a transition to a state of weak turbulence, which is subsequently dissipated over the resting period of the cardiac cycle. The transition to turbulence is stronger in non-symmetric models, since the hairpin vortex is exposed to a more intense stretching, which increases its strength.

These changes in the flow characteristics result in very large changes in the spatial and temporal distribution of the WSS acting on the endothelial cells as compared to those acting in the healthy aorta. Our measurements show the existence of two regions with distinct patterns of WSS and GWSS. The detached region is dominated by oscillatory wall shear stresses with a very low and negative average value. The reattachment region is characterized by large sustained GWSS and large negative WSS. In symmetric aneurysms, the detached region extends over the proximal half of the aneurysm and the reattachment region over the distal half. In non-symmetric aneurysms, the detached region is along the anterior wall and the reattachment region along the posterior wall.

In the shear layer and in the wall reattachment region, circulating blood cells are subjected to higher levels of shear stresses, which may cause the cells to activate and weakly aggregate. The peculiarity of aneurismal flow is indeed to transport some of the cells into the wall, right into the regions of high WSS and large gradients of WSS. This transport mechanism increases the probability of adherence of the cells to the wall at

these locations. Migration of the endothelial cells and possibly endothelial desquamation have been shown to occur along the reattachment wall, which is likely to lead to the inflammation of the vessel wall and enhance the activation processes in the circulating blood cells impinging on the wall. After their impact on the wall, the non-adhering cells are entrained into the recirculating flow regions, where they are subjected to low stresses. The cells recirculate at low speed for several cardiac cycles, being periodically subjected to higher shear stresses, each time they are brought in the vicinity of the wall at peak systole. The size and strength of the vortices shed from the proximal neck have been shown to increase as the aneurysm grows, which explains the increase in the mean shear stresses acting on the cells, as well as in the number of cells being potentially entrained into the recirculating regions. As the dilatation ratio increases, the separated flow regions also grow in size, which leads to an increase in the cell residence time. An 8-fold increase of the residence time has been measured in a medium-size symmetric aneurysm. On the contrary, increasing the aspect ratio reduces the pathological effects induced by the aneurismal dilatation. Furthermore, the persistence of the cell recirculation in the cavity throughout the cardiac cycle only occurs for dilatation ratio  $> 1.9$ . In small size aneurysms, the recirculating structures are rapidly broken down in the diastole, but they persist in larger size aneurysms. These structures are the strongest in the non-symmetric models, in which the cells move steadily at low speed for long durations inside the large recirculating zone. This exposure to low shear stresses for very long residence time is a very potent stimulus for cell activation. This activation state is reinforced by the extensive disruption of the endothelial cells caused by the very low and oscillatory wall shear stresses that rein in these detached regions. Upon activation, the mean volume of the platelets is multiplied by a factor of 8, which renders cell deposition very likely when associated with the convective flow patterns that bring the platelets in contact with the wall. However, these deposits along the walls can only be stable, if the convective forces

acting on them are weak. Thrombus formation is therefore less likely in symmetric aneurysms, where the flow reattaches to the wall during the systolic acceleration. However, we can expect thrombus to form along the anterior wall of non-symmetric aneurysm, along which the flow has been measured to be almost stagnant.

## **B. Perspectives**

**Studies of the effects of the measured stimuli on endothelial cells and circulating blood cells:** In this dissertation, the changes in the shear stresses and gradients of shear stresses have been fully characterized during the progressive enlargement of abdominal aortic aneurysms. The large body of experiments of the literature that were conducted on endothelial cells, platelets and leukocytes exposed to different stress conditions was useful to postulate possible mechanisms responsible for the growth of AAAs. However, the results of these biological studies may be questionable when applied to the abdominal aortic aneurysm, since the vast majority of the experiments have been conducted in steady flow conditions. There is therefore a need for new experiments designed under pulsatile flow conditions. The flow conditions should be varied in order to simulate the specific spatial and temporal distribution of WSS and GWSS reported here. These experiments would monitor the effects of the different patterns of hemodynamic stimuli on the cell morphology, secretions and gene expression. They should provide the much-needed information necessary to elucidate the exact role that the measured patterns of WSS have on the etiology and progression of AAAs.

**Field of platelet activation parameter:** In the dissertation, we have computed the activation parameter along the trajectory of a few blood cells. In order to get a more global picture of the locations where activation is more likely, an activation field could

be computed inside the AAA. Similarly to the cell activation parameter calculated with a relaxation time  $\Sigma$ , the activation field is transported by the following equation:

$$\frac{dA}{dt} = \tau - \frac{A}{\Sigma}, \quad (6.1)$$

where  $A$  is the activation field. The equation can also be written in the convective form:

$$\frac{\partial A}{\partial t} + u \frac{\partial A}{\partial x} + v \frac{\partial A}{\partial y} = \tau - \frac{A}{\Sigma}. \quad (6.2)$$

We have attempted to solve this equation, using an implicit scheme, based on the leap-frog method (2<sup>nd</sup> order accuracy), alternating with an Euler scheme every 15 time-steps. The initial condition at each point  $(i,j)$  inside the aneurysm, is the cell activation parameter that a particle would have after traveling through a straight tube during a certain time  $T$

$$A_0 = \frac{\Sigma}{T} \int_{t_0}^T \tau(i, j, t') e^{-t'/\Sigma} dt'. \quad (6.3)$$

Outside the aneurysm, the activation is kept equal to zero. We apply a zero flux through the sidewall, as the boundary condition and a constant flux through the exit of the aneurysm at each time steps.

Although the code is implicit, 2<sup>nd</sup> order accurate and satisfies the CFL condition, the code is unstable and diverges after a few time steps. The same equation is extensively used in research on polymers and it has been shown to be numerically stiff. It would be interesting to use some of the methods that researchers, such as Brasseur J. G. from Pennsylvania State University, developed to solve this type of equations.

**Kinetic models of activation:** The previous study would correspond to a kinetic model of activation of order zero. Kinetic models of order one could be derived in order to better understand the mechanisms of activation in AAAs. The simulation could

integrate a model of the coupling between endothelial cells, platelets and leukocytes and include the adhesive state of the walls depending on the values of the WSS and GWSS. This model could be a closer of this dissertation, since it would include all the mechanisms discussed here.

**Numerical simulations of the flow and wall shear stresses in abdominal aortic aneurysms:** It would be interesting to use the large body of experimental results in conjunction with numerical simulations of the flow in different models of AAA. The present database would help tune up the parameters of the numerical codes.



## Appendix A

# Calculations involved in post-processing of experimental data

### A. Calculation of the strain rates

From the PIV measurements of the velocity field, one can calculate the shear strain field. The derivatives of the velocity field with respect to  $y$  (parallel to the main flow direction) and  $x$  (perpendicular to the main flow direction) are discretized using centered differences, with a second order accuracy

$$\left. \frac{\partial v}{\partial x} \right|_i = \frac{v_{i+1} - v_{i-1}}{2\Delta x}, \quad (\text{A.1a})$$

$$\left. \frac{\partial u}{\partial x} \right|_i = \frac{u_{i+1} - u_{i-1}}{2\Delta x}, \quad (\text{A.1b})$$

$$\left. \frac{\partial v}{\partial y} \right|_j = \frac{v_{j+1} - v_{j-1}}{2\Delta y}, \quad (\text{A.1c})$$

$$\left. \frac{\partial u}{\partial y} \right|_j = \frac{u_{j+1} - u_{j-1}}{2\Delta y}, \quad (\text{A.1d})$$

where  $(u, v)$  are the  $x$ - and  $y$ -components of the velocity field and  $(i, j)$  the  $x$ - and  $y$ -grid position indices. The wall is placed at  $\Delta x/2$  away from the first or last grid points and the velocity at the wall is assumed to be null. The strain rates at the wall therefore read

$$\left. \frac{\partial v}{\partial x} \right|_{i \mp \Delta x/2} = \pm 2v_i / \Delta x, \quad (\text{A.2a})$$

$$\left. \frac{\partial u}{\partial x} \right|_{i \mp \Delta x/2} = \pm 2u_i / \Delta x. \quad (\text{A.2b})$$

$(u_i, v_i)$  being the velocity vector measured at the first or last grid point inside the aneurysm.

## B. Calculation of the vorticity and stress fields

From the velocity field, one can then calculate the vorticity and stress fields in the plane of measurement. The stress tensor for a Newtonian fluid can be written as

$$\sigma = \frac{1}{2} \mu [\nabla \bar{u} + \nabla \bar{u}^T]. \quad (\text{A.3})$$

In the plane of measurement, the shear stress

$$\sigma_{xy} = \frac{1}{2} \mu \left[ \frac{\partial u}{\partial y} + \frac{\partial v}{\partial x} \right] \quad (\text{A.4})$$

and vorticity

$$\omega_z = \frac{1}{2} \mu \left[ \frac{\partial v}{\partial x} - \frac{\partial u}{\partial y} \right] \quad (\text{A.5})$$

can be calculated using the previously derived expressions for the strain rates. The total stress field, as described in Appendix B, can be expressed as

$$\tau_1 = \frac{1}{2} \mu \left( \frac{\partial u}{\partial x} + \frac{\partial v}{\partial y} \right) + \frac{1}{2} \mu \left[ \left( \frac{\partial u}{\partial x} - \frac{\partial v}{\partial y} \right)^2 + \left( \frac{\partial u}{\partial y} + \frac{\partial v}{\partial x} \right)^2 \right]^{0.5}. \quad (\text{A.6})$$

### C. Calculation of the wall shear stresses

The wall shear stress is defined as

$$WSS = 2\mu(\sigma \cdot \vec{n}) \cdot \vec{t}, \quad (\text{A.7})$$

$\vec{n}$  and  $\vec{t}$  being respectively the normal and tangential unit vectors. In Cartesian two-dimensional coordinates, the WSS takes the form

$$WSS = 2\mu[\sigma_{xy}(n_x^2 - n_y^2) + (\sigma_{yy} - \sigma_{xx})n_x n_y]. \quad (\text{A.8})$$

In order to calculate the wall shear stresses, one needs to estimate the local normal unit vector  $\vec{n}$ . In the case of the healthy abdominal aorta, modeled in this study as a straight tube, it is equal to  $\vec{n} = (1,0)$ . Inside the abdominal aortic aneurysm, the shape of the aneurysm was approximated by a cosine function

$$a(y) = a_0 + \frac{1}{2} \left( \frac{D}{2} - a_0 \right) \left[ 1 + \cos \left( \frac{2\pi(y - L/2)}{L} \right) \right]. \quad (\text{A.9})$$

The unit normal vector therefore reads

$$n_x = \pm \frac{1}{\sqrt{1 + (da/dy)^2}}, \quad (\text{A.10a})$$

$$n_y = \mp \frac{da/dy}{\sqrt{1 + (da/dy)^2}}. \quad (\text{A.10b})$$



## Appendix B

### Calculation of the total stress

The total stress, as referred to in this paper, is defined as the maximum eigenvalue of the stress tensor (A.3), which admits the following eigenvalues

$$\tau_1 = \frac{1}{2} \mu \left( \frac{\partial u_r}{\partial r} + \frac{\partial u_z}{\partial z} \right) + \frac{1}{2} \mu \left[ \left( \frac{\partial u_r}{\partial r} - \frac{\partial u_z}{\partial z} \right)^2 + \left( \frac{\partial u_r}{\partial z} + \frac{\partial u_z}{\partial r} \right)^2 \right]^{0.5}, \quad (\text{B.1a})$$

$$\tau_2 = \frac{1}{2} \mu \left( \frac{\partial u_r}{\partial r} + \frac{\partial u_z}{\partial z} \right) - \frac{1}{2} \mu \left[ \left( \frac{\partial u_r}{\partial r} - \frac{\partial u_z}{\partial z} \right)^2 + \left( \frac{\partial u_r}{\partial z} + \frac{\partial u_z}{\partial r} \right)^2 \right]^{0.5}, \quad (\text{B.1b})$$

$$\tau_3 = \mu \frac{u_r}{r}, \quad (\text{B.1c})$$

when expressed in the  $(r, \theta, z)$  coordinate system. The total stress is set equal to  $\tau_1$ . Upon changing the variables from a cylindrical to a Cartesian coordinate system, the stress in the symmetry plane of the aneurysm model can be expressed by equation (A.6). This measurement of the stresses has the advantage upon the shear stresses to be invariant with respect to an arbitrary rotation of the coordinate axes.



## Appendix C

### Manufacture of silicone models of anatomically correct abdominal aortic aneurysms

The flow characteristics inside an anatomically correct AAA are shown at the end of the results in chapter 4. The model is reconstructed from a set of high-resolution images obtained with a GE helical CT scanner (Figure C.1). A three-dimensional reconstruction of the geometry of the lumen is first generated from the CT scan images using a volume rendering technique (Figure C.2 (a)). A model of the in vivo aneurysm is then manufactured through rapid-prototyping (Figure C.2 (b)). The mold, made out of plaster of Paris, is an exact replica of the whole arterial trunk spanning from 10 cm upstream of the renal arteries to 5 cm downstream of the iliac bifurcation. An elastic model, made of optically clear silicone, is created using a lost wax technique (Figure C.2 (c)). The mold is first coated with a very thin layer of wax in order to make the mold impermeable and then with silicone. The thickness of the silicone layer is kept as uniform as possible. The dissolution of the mold leaves an anatomically correct model of the whole arterial system that includes all the major arterial bifurcations (bifurcations to the renal, mesenteric and iliac arteries).

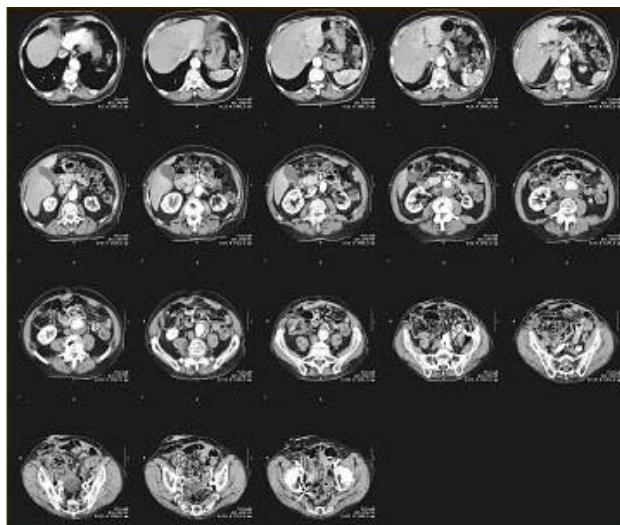


Figure C.1: CT scan images of the abdominal trunk of a patient with an AAA.

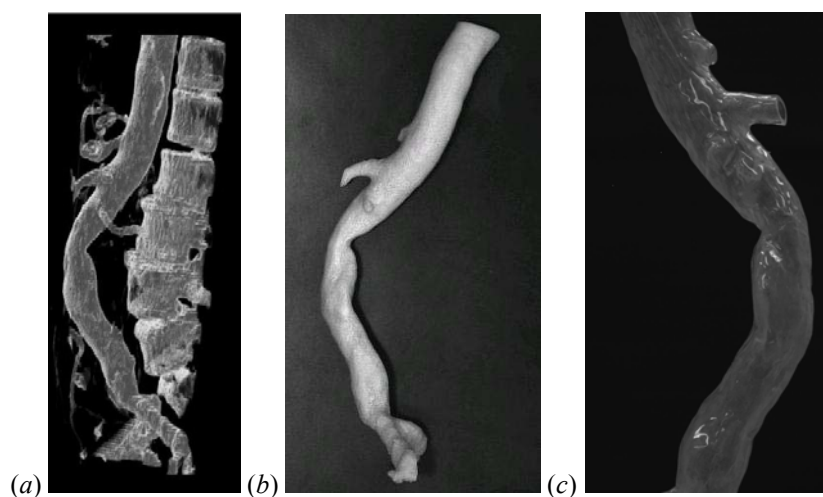


Figure C.2: (a) Three-dimensional reconstruction of an AAA from CT scan images, (b) mold generated in plaster of Paris with a rapid prototyping technique, (c) silicone model built from the mold using a lost wax technique.

## REFERENCES

- The UK Small Aneurysm Trial Participants. "Smoking, lung function and the prognosis of abdominal aortic aneurysm." *Eur. J. Vasc. Endovasc. Surg.* **19**, 636–642 (2000).
- Adolph R., Vorp D. A., Steed D. L., Webster M. W., Kameneva M. V. & Watkins S. C. "Cellular content and permeability of intraluminal thrombus in abdominal aortic aneurysm." *J. Vasc. Surg.* **25**, 916–926 (1997).
- Alveriadou B. R., Moake J. L., Turner N. A., Ruggeri Z. M., Folie B. J., Phillips M. D., Schreiber A. B., Hrinda M. E. & McIntire L. V. Real-time analysis of shear dependent thrombus formation and its blockade by inhibitors of Van Willebrand factors binding to platelets. *Blood.* **81**, 1263-1276 (1993).
- Andrews R. K., Shen Y., Gardiner E. E. & Berndt M. C. "Platelet adhesion receptors and (patho)physiological thrombus formation." *Histol. Histopathol.* **16**, 969–980 (2001).
- Armon M. P., Wenham P. W., Whitaker S. C., Gregson R. H. S. & Hopkinson B. R. "Common iliac artery aneurysms in patients with abdominal aortic aneurysms." *Eur. J. Vasc. Endovasc. Surg.* **15**, 255–257 (1998).
- Asbury C. L., Ruberti J. W., Bluth E. I. & Peattie R. A. "Experimental investigation of steady flow in rigid models of abdominal aortic aneurysms." *Ann. Biomed. Eng.* **23**, 23–39 (1995).
- Auerbach O. & Garfinkel L. "Atherosclerosis and aneurysm of the aorta in relation to smoking habits and age." *Chest.* **78**, 805–809 (1980).
- Bao X., Lu C. & Frangos J. a. "Temporal gradient in shear but not steady shear stress induces PDGF-A and MCP-1 expression in endothelial cells; Role of NO, NFκB and *egr-1*." *Arteriosclr. Thromb. Vasc. Biol.* **19**, 996–1003 (1999).
- Basnyat P. S., Biffin A. H. B., Moseley L. G., Hedges A. R. & Lewis M. E. "Mortality from ruptured abdominal aortic aneurysm in Wales." *Br. J. Surg.* **86**, 765–770 (1999).
- Bassiouny H. S., Song R. H., Kocharyan H., Kins E. & Glagov S. "Low flow enhances platelet activation after acute experimental arterial injury." *J. Vasc. Surg.* **27**, 910–918 (1998).

- Baumgartner H. R., Tschopp T. B. & Meyer D. "Shear rate dependent inhibition of platelet adhesion and aggregation on collagenous surfaces by antibodies to human factor VIII/von Willebrand factor." *Br. J. Haematol.* **44**, 127–139 (1980).
- Baumgartner H. R., Turitto V. & Weiss H. J. "Effects of shear rate on platelet interaction with subendothelium in citrated and native blood. II. Relationships among platelet adhesion, thrombus dimensions, and fibrin formation." *J. Lab. Clin. Med.* **95**, 208–221 (1980).
- Ben Driss A., Benessiano J., Poitevin P., Levy B. I. & Michel J. B. "Arterial expansive remodeling induced by high flow rates." *Am. J. Physiol.* **272**, H851–H858 (1997).
- Bengtsson H., Sonesson B. & Bergqvist D. "Incidence and prevalence of abdominal aortic aneurysms, estimated by necropsy studies and population screening by ultrasound." In *The abdominal aortic aneurysm: genetics, pathophysiology, and molecular biology* (ed. Tilson M. D. & Boyd C. D.) New York, N. Y. New York Academy of Sciences (1996).
- Best A., Price J. F. & Fowkes F. G. R., "Persistent increase in the incidence of abdominal aortic aneurysm in Scotland, 1981-2000." *Brit. J. Surg.* **90**, 1510–1515 (2003).
- Blackman B. R., Thibault L. E. & Barbee K. A. "Selective modulation of endothelial cell  $[Ca^{2+}]_i$  response to flow by the onset rate of shear stress." *J. Biomech. Eng.* **122**, 274–282 (2000).
- Blackman B. R., García-Cardena G. & Gimbrone M. A. Jr. "A new in vitro model to evaluate differential responses of endothelial cells to simulated arterial shear stress waveforms." *J. Biomech. Eng.* **124**, 397–407 (2002).
- Bluestein D., Niu L., Schoepfoerster R. T. & Dewanjee M. K. "Steady flow in an aneurysm model: correlation between fluid dynamics and blood platelet deposition." *J. Biomech. Eng.* **118**, 280–286 (1996).
- Bluestein D., Rambod E. & Gharib M. "Vortex shedding as a mechanism for free emboli formation in mechanical heart valves." *J. Biomech. Eng.* **122**, 125-134 (2000).
- Bluestein D., Yin W., Affeld K. & Jesty J. "Flow-induced platelet activation in mechanical heart valves." *J. Heart Valve Dis.* **13**, 501–508 (2004).
- Bonamigo T. P. & Siqueira I. "Screening for abdominal aortic aneurysms." *Rev. Hosp. Clin. Fac. Med. Sao Paulo.* **58**, 63–68 (2003).
- Budwig R., Elger D., Hooper H. & Slippery J. "Steady flow in abdominal aortic aneurysm models." *J. Biomech. Eng.* **115**, 418–423 (1993).

- Busuttil R. W., Abou-Zamzam A. M. & Machkeder H. L. "Collagenase activity of the human aorta: comparison of patients with and without abdominal aortic aneurysms." *Arch. Surg.* **115**, 1373–1378 (1980).
- Busuttil R. W., Rinderbriecht J., Flesher A. & Carmack C. "Elastase activity: the role of elastase in aneurysm formation." *Surg. Res.* **32**, 214–217 (1982).
- Carmo M., Columbo L., Bruno A., Corsi F. R., Roncoroni L., Cuttin M. S., Radice F., Mussini E. & Settembrini P. G. "Alteration of elastin, collagen and their cross-links in abdominal aortic aneurysms." *Eur. J. Vasc. Endovasc. Surg.* **23**, 543–549 (2002).
- Caro C. G. *et al.* *The Mechanics of the Circulation*. Oxford, Oxford University Press (1978).
- Caro C. G., Fitz-Gerald J. M. & Schroter R. C. "Atheroma and arterial wall shear: observation, correlation and proposal of a shear dependent mass transfer mechanism for atherogenesis." *Proc. R Soc. Lond. B Biol. Sci.* **177**, 109–159 (1971).
- Chappell D. C., Varner S. E., Nerem R. M., Medford R. M. & Alexander R. W. "Oscillatory shear stress stimulates adhesion molecule expression in cultured human endothelium." *Circ. Res.* **82**, 532–539 (1998).
- Chaudhuri A., Ansdell L. E., Grass A. J. & Adiseshiah M. "Aneurysmal hypertension and its relationship to sac thrombus: a semi-qualitative analysis by experimental fluid mechanics." *Eur. J. Vasc. Endovasc. Surg.* **27**, 305–310 (2004).
- Cheng C. P., Parker D. & Taylor C. A. "Quantification of wall shear stress in large blood vessels using Lagrangian interpolation functions with cine phase-contrast magnetic resonance imaging." *Ann. Biomed. Eng.* **30**, 1020–1032 (2002).
- Chiu J. J., Chen L. J., Chen C. N., Lee P. L. & Lee C. I. "A model for studying the effect of shear stress on interactions between vascular endothelial cells and smooth muscle cells." *J. Biomech.* **37**, 531–539 (2004).
- Chiu J. J., Chen L. J., Lee P. L., Lee C. I., Lo L.W., Usami S. & Chien S. "Shear stress inhibits adhesion molecule expression in vascular endothelial cells induced by coculture with smooth muscle cells." *Blood.* **101**, 2667–2674 (2003).
- Chow T. W., Hellums J. D., Moake J. L. & Kroll M. H. "Shear stress-induced von Willebrand factor binding to platelet glycoprotein Ib initiates calcium influx associated with aggregation." *Blood.* **1**, 113–120 (1992).
- Collin, J. & Radcliffe, J., "The epidemiology of abdominal aortic aneurysms." *Br. J. Hosp. Med.* **7**, 64–67 (1988).

- Cucina A., Sterpetti A. V., di Carlo A., Randone B., Aromatario C., Proietti P., Giustiniani Q., Cavallaro A. & Santoro-D'Angelo L. "Hemodynamic forces modulate simultaneously the release of growth factors and the organization of cytoskeleton of aortic smooth muscle cells." *Minerva Cardioangiol.* **44**, 637–643 (1996).
- Darling R. C. "Ruptured arteriosclerotic abdominal aortic aneurysms." *Am. J. Surg.* **119**, 397–401 (1970).
- David T., Thomas S. & Walker P. G. "Platelet deposition in stagnation point flow: an analytical and computational simulation." *Med. Eng. Phys.* **23**, 299–312 (2001).
- Davies P. F., Dewey C. F., Bussolari S., Gordon E. & Gibrone M. A. "Influence of hemodynamic forces on vascular endothelial function." *J. Clin. Invest.* **73**, 1121–1129 (1984).
- Davies P. F., Mundel T. & Barbee K. A. "A mechanism for heterogeneous endothelial responses to flow *in vivo* and *in vitro*." *J. Biomech.* **28**, 1553–1560 (1995).
- Davies P. F., Remuzzi A., Gordon E. J., Dewey C. F. Jr & Gibrone M. A. Jr. "Turbulent fluid shear stress induces vascular endothelial turnover *in vitro*." *Proc. Natl. Acad. Sci. USA.* **83**, 2114–2117 (1986).
- DePaola N., Gimbrone M., Davies P. & Dewey C. "Vascular endothelium responds to fluid shear stress gradients." *Arterioscl. Thromb.* **12**, 1254–1257 (1992).
- Dewey C., Bussolari S., Gimbrone M. & Davies P. "The dynamic response of vascular endothelial cells to fluid shear stress." *J. Biomech. Eng.* **103**, 177–185 (1981).
- Di Martino E., Mantero S., Inzoli F., Melissano G., Astore D., Chiesa R. & Fumero R. "Biomechanics of abdominal aortic aneurysm in the presence of endoluminal thrombus: experimental characterization and structure static computational analysis." *Eur. J. Vasc. Endovasc. Surg.* **15**, 290–299 (1998).
- Di Martino E. S., Guadagni G., Fumero A., Ballerini G., Spirito R., Biglioli P. & Redaelli A. "Fluid-structure interaction within realistic three-dimensional models of the aneurysmatic aorta as a guidance to assess the risk of rupture of the aneurysm." *Med. Eng. Phys.* **23**, 647–655 (2001)
- Dintenfass L. "Rheological approach to thrombosis and atherosclerosis." *Angiology.* **15**, 333–343 (1964).
- Dobrin P. B. "Pathophysiology and pathogenesis of aortic aneurysms." In *Abdominal aortic aneurysms* (ed. Pierce G. E.) Philadelphia: Saunders, 687–703 (1989).

- Egelhoff C. J., Budwig R. S., Elger D. F., Khraishi T. A. & Johansen K. H. "Model studies of the flow in abdominal aortic aneurysms during resting and exercise conditions." *J. Biomech.* **32**, 1319–1329 (1999).
- Einav S. & Bluestein D. "Dynamics of blood flow and platelet transport in pathological vessels." *Ann. N. Y. Acad. Sci.* **1015**, 351-366 (2004).
- Emerson M., Momi S., Paul W., Alberti P. F., Page C. & Gresele P. "Endogenous nitric oxide acts as a natural antithrombotic agent in vivo by inhibiting platelet aggregation in the pulmonary vasculature." *Thromb. Haemost.* **81**, 961-966 (1999).
- Englund R., Hudson P., Hanel K. & Stanton A. "Expansion rates of small abdominal aortic aneurysms." *Aust. N. Z. J. Surg.* **123**, 474–484 (1998).
- Eriksson E. E., Zerr J., Guo Y., Thoren P. & Lindbom L. "Direct observations in vivo on the role of endothelial selectins and  $\alpha_4$  integrin in cytokine-induced leukocyte-endothelium interactions in the mouse aorta." *Circ. Res.* **86**, 526-533 (2000).
- Finol E. A. & Amon C. H. "Blood flow in abdominal aortic aneurysms: pulsatile flow hemodynamics." *J. Biom. Eng.* **123**, 474–484 (2001).
- Finol<sup>1</sup> E. A. & Amon C. H. "Flow-induced Wall Shear Stress in Abdominal Aortic Aneurysms: Part I – Steady Flow Hemodynamics." *Comput. Methods Biomech. Biomed. Engin.* **5**, 309–318 (2002).
- Finol<sup>2</sup> E. A. & Amon C. H. "Flow-induced Wall Shear Stress in Abdominal Aortic Aneurysms: Part II - Pulsatile Flow Hemodynamics." *Comput. Methods Biomech. Biomed. Engin.* **5**, 319–328 (2002).
- Finol E. A. & Amon C. H. "Flow dynamics in abdominal aortic aneurysms." *Acta Cient. Venez.* **54**, 43–49 (2003).
- Fisher A. B., Chien S., Barakat A. I. & Nerem R. M., "Endothelial cellular response to altered shear stress." *Am. J. Physiol. Lung Cell Mol. Physiol.* **281**, L529-L533 (2001).
- Folie B. J. & McIntire L. V. "Mathematical analysis of mural thrombogenesis. Concentration profiles of platelet-activating agents and effects of viscous shear flow." *Biophys. J.* **56**, 1121–1141 (1989).
- Fontaine V., Jacob M.-P., Rossignol P., Plissonnier D., Angles-Cano E. & Michel J.-B. "Involvement of the mural thrombus as a site of protease release and activation in human aortic aneurysms." *Am. J. Pathol.* **161**, 1701–1710 (2002).
- Forlow S. B., McEver R. P. & Nollert M. U. "Leukocyte-leukocyte interactions mediated by platelet microparticles under flow." *Blood.* **95**, 1317-1323 (2000).

- Fox J. A. & Hugh A. E. "Localization of atheroma: a theory based on boundary layer separation." *Br. Heart J.* **26**, 388–399 (1966).
- Fukuda S., Yasu T., Predescu D. N. & Schmid-Schoenbein G. W. "Mechanisms for regulation of fluid shear stress response in circulating leukocytes." *Circ. Res.* **86**, e13-e18, 2000.
- Fukushima T., Matsuzawa T. & Homma T. "Visualization and finite element analysis of pulsatile flow in models of the abdominal aortic aneurysm." *Biorheology* **26**, 109–130 (1989).
- Gacko M. & Głowiński S. "Activities of proteases in parietal thrombus of aortic aneurysm." *Clin. Chim. Acta.* **271**, 171–177 (1998).
- García-Cardena<sup>1</sup> G., Comander J. I., Anderson K. R., Blackman B. R. & Gimbrone M. A. Jr. "Biomechanical activation of vascular endothelium as a determinant of its functional phenotype." *Proc. Natl. Acad. Sci. USA.* **10**, 4478–4485 (2001).
- García-Cardena<sup>2</sup> G., Comander J. I., Blackman B. R., Anderson K. R. & Gimbrone M. A. "Mechanosensitive endothelial gene expression profiles: scripts for the role of hemodynamics in atherogenesis?" *Ann. N. Y. Acad. Sci.* **947**, 1–6 (2001).
- Gharib M., Rambod E. & Shariff K. "A universal time scale for vortex ring formation." *J. Fluid Mech.* **360**, 121–140 (1998).
- Ghorpade A. & Baxter B. T. "Biochemistry and molecular regulation of matrix macromolecules in abdominal aortic aneurysms." In *The abdominal aortic aneurysm: genetics, pathophysiology, and molecular biology* (ed. Tilson M. D. & Boyd C. D.) New York, N. Y. New York Academy of Sciences (1996).
- Glagov S., Zarins C. K., Giddens D. G. & Ku D. N. "Hemodynamics and atherosclerosis, insights and perspectives gained from studies of human arteries." *Arch. Pathol. Lab. Med.* **112**, 1018–1031 (1988).
- Goldsmith H. L. "Blood flow and thrombosis." *Thromb. Diath Haemorrh.* **32**, 35–48 (1974).
- Gosgnach W., Messika-Zeitoun D., Gonzalez W., Philippe M. & Michel J.-B. "Shear stress induces iNOS expression in cultured smooth muscle cells: role of oxidative stress." *Am. J. Physiol. Cell Physiol.* **279**, C1880-C1888 (2000).
- Grabowski E. F. "Thrombolysis, flow, and vessel wall interactions." *J. Vasc. Interv. Radiol.* **6**, 25S-29S (1995).
- Green R. M. "Patient selection for endovascular AAA repair." *Endovascular Today.* **6**, 31-33 (2002).

- Greenwald S. E., Carter A. C. & Berry C. L. “Effect of age on the in vitro reflection coefficient of the aortoiliac bifurcation in humans.” *Circulation*. **82**, 114–123 (1990).
- Hardy-Stashin J., Meyer W. W. & Kauffman S. L. “Branching coefficient (“area ratio”) of the human aortic bifurcation determined in distended specimens.” *Atherosclerosis*. **37**, 399–402 (1980).
- Harter L. P., Gross B. H., Callen P. W. & Barth R. A. “Ultrasonic evaluation of abdominal aortic thrombus.” *J. Ultrasound Med.* **1**, 315–318 (1982).
- Hatakeyama T., Shigematsu H. & Muto T. “Risk factors for rupture of abdominal aortic aneurysm based on three-dimensional study.” *J. Vasc. Surg.* **33**, 453–461 (2001).
- He C. M. & Roach M. R. “The composition and mechanical properties of abdominal aortic aneurysms.” *J. Vasc. Surg.* **20**, 6–13 (1994).
- Heldin C. H. & Westermark B. “Mechanism of action and in vivo role of platelet-derived growth factor,” *Physiol. Rev.* **79**, 1283–1316 (1999).
- Hellums J. D. & Hardwick R. A. “Response of platelets to shear stress – a review.” *The Rheology of blood, blood vessels and associated tissues* (ed. Hwang N. H. C. & Gross D. R.) Sijthoff and Noorhoff, Amsterdam. 160–183 (1981).
- Helmlinger G., Geiger R. V., Schreck S. & Nerem R. M. “Effects of pulsatile flow on cultured vascular endothelial cell morphology.” *J. Biomech. Eng.* **113**, 123–131 (1991).
- Helmlinger G., Berk B. C. & Nerem R. M. “Calcium responses of endothelial cell monolayers subjected to pulsatile and steady laminar flow differ.” *Am. J. Physiol.* **269**, C367–C375 (1995).
- Helps E. P. & McDonald D. A. “Arterial blood flow calculated from pressure gradients.” *J. Physiol.* **124**, 30–1P (1954).
- Hernandez M. R., Bozzo J., Tonda R., Galan A. M., Ordinas A. & Escolar G. “Effect of anticoagulants on activation of polymorphonuclear leukocytes induced by shear stress.” *Int. J. Immunopathol. Pharmacol.* **14**, 139 (2001).
- Holenstein R. & Ku D. N. “Reverse flow in the major infrarenal vessels – a capacitive phenomenon.” *Biorheology*. **25**, 835–842 (1988).
- Hsiai T. K., Cho S. K., Honda H. M., Hama S., Navab M., Demer L. L. & Ho C.-M. “Endothelial cell dynamics under pulsating flows: significance of high versus low shear stress slew rates ( $\partial\tau/\partial t$ ).” *Ann. Biomed. Eng.* **30**, 646–656 (2002).

- Huang P. Y. & Hellums J. D. "Aggregation and disaggregation kinetics of human blood platelets: Part I, II and III." *Biophys. J.* **65**, 334–343 (1993).
- Hughes M. L. & Fontenelle L. J. "A 5-year review of abdominal aortic aneurysms at a VA medical center." *Curr. Surg.* **57**, 343–345 (2000).
- Ikeda Y., Handa M., Kawano K., Kamata T., Murata M., Araki Y., Anbo H., Kawai Y., Watanabe K., Itagaki I., Sakai K. & Ruggeri Z. M. "The role of von Willebrand factor and fibrinogen in platelet aggregation under varying shear stress." *J. Clin. Invest.* **87**, 1234–1240 (1991).
- Ikeda Y., Handa M., Kamata T., Kawano K., Kawai Y., Watanabe K., Kawakami K., Sakai K., Fukuyama M., Itagaki I., Yoshioka A. & Ruggeri Z. M. "Transmembrane calcium influx associated with von Willebrand factor binding to GP Ib in the initiation of shear-induced platelet aggregation." *Thromb. Haemost.* **69**, 496–502 (1993).
- Ingoldby C. J. H., Wujanto R. & Mitchell J. E. "Impact of vascular surgery on community mortality from ruptured aortic aneurysms." *Br. J. Surg.* **73**, 551–553 (1986).
- Inzoli F., Boschetti F., Zappa M., Longo T. & Fumero R. "Biomechanical factors in abdominal aortic aneurysm rupture." *Eur. J. Vasc. Surg.* **7**, 667–674 (1993).
- Izzo J. L. & Shykoff B. E. "Arterial stiffness: clinical relevance, measurement and treatment." *Rev. Cardiovasc. Med.* **2**, 29–40 (2001).
- Jesty J., Yin W., Perrotta P. & Bluestein D. "Platelet activation in a circulating flow loop: combined effects of shear stress and exposure time." *Platelets.* **14**, 143–149 (2003).
- Johansen K., "Aneurysm." *Sci. Am.* **247**, 110–125 (1982).
- Johnston K. W., Rutherford R. B., Tilson M. D. Shah D. M. Hollier L., Stanley J. C. "Suggested standards for reporting on arterial aneurysms. Subcommittee on reporting standards for arterial aneurysms, ad hoc committee on reporting standards, Society for Vascular Surgery and North American Chapter, International Society for Cardiovascular Surgery." *J. Vasc. Surg.* **13**, 452–458 (1991).
- Kamiya A. & Togawa T. "Adaptative regulation of wall shear stress to flow change in the canine carotid artery." *Am. J. Physiol.* **239**, H14–21 (1980).
- Karino T. & Goldsmith H. L. "Role of blood cell-wall interactions in thrombogenesis and atherogenesis: a microrheological study." *Biorheology.* **21**, 587–601 (1984).

- Kazi M., Thyberg J., Religa P., Roy J., Eriksson P., Hedin U. & Swedenborg J. "Influence of intraluminal thrombus on structural and cellular composition of abdominal aortic aneurysm wall." *J. Vasc. Surg.* **38**, 1283–1292 (2003).
- Kraiss L. W., Geary R. L., Mattsson E. J., Vergel S., Au A. Y., Clowes A. W. "Acute reductions in blood flow and shear stress induce platelet-derived growth factor-A expression in baboon prosthetic grafts." *Circ. Res.* **79**, 45–53 (1996).
- Kroll M. H., Hellums J. D., McIntire L. V., Schafer A. L. & Moake J. L. "Platelets and shear stress." *Blood* **88**, 1525–1541 (1996).
- Ku D. N. & Zhu C. "The mechanical environment of the artery." In *Hemodynamic forces and vascular cell biology* (ed. Sumpio B.) Austin, Landes Co. (1997).
- Ku D. N., Giddens D. P., Zarins C. K. & Glagov S. "Pulsatile flow and atherosclerosis in the human carotid bifurcation. Positive correlation between plaque location and low oscillating shear stress." *Arteriosclerosis*. **5**, 293–302 (1985).
- Kunov M. J., Steinman D. A. & Ethier C. R. "Particle volumetric residence time calculations in arterial geometries." *J. Biomech. Eng.* **118**, 158-164 (1996).
- Law M. R., Morris J. & Wald N. J. "Screening for abdominal aortic aneurysms." *J. Med. Screen.* **1**, 110–116 (1994).
- Lawrence M. B., Kansas G. S., Kundel E. J. & Ley K. "Threshold levels of fluid shear promote leukocyte adhesion through selectins (CD62L,P,E)." *J. Cell Biol.* **136**, 717-727 (1997).
- Lee A. A., Graham D. A., Dela Cruz S., Ratcliffe A., Karlon W. J. "Fluid shear stress-induced alignment of cultured vascular smooth muscle cells." *J. Biomech. Eng.* **124**, 37–43 (2002).
- Lee A. J., Flowkes F. G., Carson M. N., Leng G. C. & Allan P. L. "Smoking, atherosclerosis and risk of abdominal aortic aneurysm." *Eur. Heart. J.* **18**, 545–546 (1997).
- Lee D., Chiu Y. L. & Jen C. Y. "Wall stresses and platelet adhesion in a T-junction." *Proc. Natl. Sci. Counc. ROC(A)*. **23**, 303–310 (1999).
- Lee R. T., Yamamoto C., Feng Y., Potter-Perigo S., Briggs W. H., Landschulz K. T., Turi T. G., Thompson J. F., Libby P. & Wight T. N. "Mechanical strain induces specific changes in the synthesis and organization of proteoglycans by vascular smooth muscle cells." *J. Biol. Chem.* **276**, 13847–13851 (2001).
- Lei M., Kleinstueber C. & Truskey G. A. "Numerical investigation and prediction of atherogenic sites in branching arteries." *J. Biomech. Eng.* **117**, 350–357 (1995).

- Levesque M. J. & Nerem R. M., “The elongation and orientation of cultured endothelial cells in response to shear stress.” *J. Biomech. Eng.* **107**, 341–347 (1985).
- Liao S., Curci J. A., Kelley B. J., Sicard G. A. & Thompson R. W., “Accelerated replicative senescence of medial smooth muscle cells derived from abdominal aortic aneurysms compared to the adjacent inferior mesenteric artery.” *J. Surg. Res.* **92**, 85–95 (2000).
- Limas C., Westrum B. & Limas C. J. “The evolution of vascular changes in the spontaneously hypertensive rat.” *Am. J. Pathol.* **98**, 357–384 (1980).
- Long Q., Xu X. Y., Bourne M. & Griffith T. M. “Numerical study of blood flow in an anatomically realistic aorto-iliac bifurcation generated from MRI data.” *Magn. Reson. Med.* **43**, 565–576 (2000).
- Longest P. W. & Kleinstuever C. “Numerical simulation of wall shear stress conditions and platelet localization in realistic end-to-side arterial anastomoses.” *J. Biomech. Eng.* **125**, 671–681 (2003).
- López-Candales A., Holmes D. R., Liao S., Scott M. J., Wickline S. A. & Thompson R. W. “Decreased vascular smooth muscle cell density in medial degeneration of human abdominal aortic aneurysms.” *Am. J. Pathol.* **150**, 993–1007 (1997).
- MacSweeney S. T., Young G., Greenhalgh R. M. & Powell J. T. “Mechanical properties of the aneurysmal aorta.” *Br. J. Surg.* **79**, 1281–1284 (1992).
- MacSweeney, S. T. R. “Abdominal aortic aneurysms.” In *Pathophysiology of aneurysm disease – Report of a meeting of physicians and scientists*. London: University College London Medical School. *Lancet.* **341**, 215–220 (1993).
- MacSweeney, S. T. R., Ellis M., Worrell P. C., Greenhalgh R. M. & Powell J. T. “Smoking and growth rate of small abdominal aortic aneurysms.” *Lancet.* **344**, 651–652 (1994).
- Maier S. E., Meier D., Boesinger P., Moser U. T. & Vieli A. “Human abdominal aorta: comparative measurements of blood flow with MR imaging and multigated Doppler US.” *Radiology* **171**, 487–492 (1989)
- Mailhac A., Badimon J. J., Fallon J. T., Fernandez-Ortiz A., Meyer B., Chesebro J. H., Fuster V. & Badimon L. “Effect of an eccentric severe stenosis on fibrin(ogen) deposition on severely damaged vessel wall in arterial thrombosis. Relative contribution of fibrin(ogen) and platelets.” *Circulation.* **90**, 988–996 (1994).
- Malek M., Alper S. L. & Izumo S. “Hemodynamic shear stress and its role in atherosclerosis.” *JAMA.* **282**, 2035–2042 (1999).

- Marschel P. & Schmid-Schoenbein G. W. "Control of fluid shear response in circulating leukocytes by integrins." *Ann. Biomed. Eng.* **30**, 333-343 (2002).
- Matsushita M., Nishikimi N., Sakurai T., Nimura Y. "Relationship between aortic calcification and atherosclerotic disease in patients with abdominal aortic aneurysm." *Int. Angiol.* **19**, 276-279 (2000).
- McDonald D. A. *Blood flow in arteries*. Baltimore, Williams & Wilkens (1974).
- Mills C. J., Gabe I. T., Gault J. H., Mason D. T., Ross J., Braunwald E. & Shillingford J. P. "Pressure-flow relationships and vascular impedance in man." *Cardiovasc. Res.* **4**, 405-417 (1970)
- Moake J. L., Turner N. A., Stathopoulos N. A., Nolasco L. H. & Hellums J. D. "Involvement of large plasma von Willebrand factor (vWF) multimers and unusually large vWF forms derived from endothelial cells in shear stress-induced platelet aggregation." *J. Clin. Invest.* **78**, 1456-1461 (1986).
- Moazzam F., DeLano F. A., Zweifach B. W. & Schmid-Schoenbein G. W. "The leukocyte response to fluid stress." *Proc. Natl. Acad. Sci. USA.* **94**, 5338-5343 (1997).
- Moore J. E., Ku K. D., Zarins C. K. & Glagov S. "Pulsatile flow visualization in the abdominal aorta under differing physiologic conditions: implications for increased susceptibility to atherosclerosis." *J. Biomech. Eng.* **114**, 391-397 (1992).
- Moore J. E., Xu C., Glagov S., Zarins C. K. & Ku D. N. Fluid wall shear stress measurements in a model of the human abdominal aorta: oscillatory behavior and relationship to atherosclerosis. *Atherosclerosis.* **110**, 225-240 (1994).
- Mower W. R., Quinones W. J. & Gambhir S. S. "Effect of intraluminal thrombus on abdominal aortic aneurysm wall stress." *J. Vasc. Surg.* **26**, 602-608 (1997).
- Mower W. R. & Quinones W. J. "Regarding "thrombus within an aortic aneurysm does not reduce the pressure on the aneurysm wall."" *J. Vasc. Surg.* **33**, 660-661 (2001).
- Nagel T., Resnick N., Dewey C. F. & Gimbrone M. A. "Vascular endothelial cells respond to spatial gradients in fluid shear stress by enhanced activation of transcription factors." *Arterioscl. Thromb. Vasc. Biol.* **19**, 1825-1834 (1999).
- Nichols W. W. *McDonald's blood flow in arteries: theoretic, experimental and clinical principles* (ed. Nichols W.W. & O'Rourke M. F.) London, Arnold (1998).
- Nomura S., Tandon N. N., Nakamura T., Cone J., Fukuhara S. & Kambayashi J. "High-shear-stress-induced activation of platelets and microparticles enhances

expression of cell adhesion molecules in THP-1 and endothelial cells.” *Atherosclerosis*. **158**, 277-287 (2001).

Noorgard O., Rais O. & Angquist K. A. “Familial occurrence of abdominal aortic aneurysms.” *Surgery*. **95**, 650-656 (1984).

Noris M., Morigi M., Donadelli R., Aiello S., Foppolo M., Todeschini M., Orisio S., Remuzzi G. & Remuzzi A. “Nitric oxide synthesis by cultured endothelial cells is modulated by flow conditions.” *Circ. Res.* **76**, 536-543 (1995).

O’Brien J. R. “Shear-induced platelet aggregation.” *Lancet*. **335**, 711-713 (1990).

Okuyama M. Ohta Y., Kambayashi J. & Monden M. “Fluid shear stress induces actin polymerization in human neutrophils.” *J. Cell Biochem.* **63**, 434-441 (1996).

O’Rourke M., Arterial stiffness, systolic blood pressure and logical treatment of arterial hypertension.” *Hypertension*. **15**, 339-347 (1990).

Oyre S., Pedersen E. M., Ringgaard S., Boesiger P. & Paaske W. P. “*In vivo* wall shear stress measured by magnetic resonance velocity mapping in the normal human abdominal aorta.” *Eur. J. Vasc. Endovasc. Surg.* **13**, 263-271 (1997).

Paivansalo M. J., Merikanto J., Jerkkola T., Savolainen M. J., Rantala A. O., Kauma H., Lilja M., Reunanen Y. A., Kesaniemi A. & Suramo I. “Effect of hypertension and risk factors on diameters of abdominal aorta and common iliac and femoral arteries in middle-aged hypertensive and control subjects: a cross-sectional systematic study with duplex ultrasound.” *Atherosclerosis*. **153**, 99-106 (2000).

Papadaki<sup>1</sup> M., Ruef J., Nguyen K. T., Li F., Patterson C., Eskin S. G., McIntire L. V. & Runge M. S. “Differential regulation of protease activated receptor-1 and tissue plasminogen activator expression by shear stress in vascular smooth muscle cells.” *Circ. Res.* **83**, 1027-1034 (1998).

Papadaki<sup>2</sup> M., Tilton R. G., Eskin S. G. & McIntire L. V. “Nitric oxide production by cultured human aortic smooth muscle cells: stimulation by fluid flow.” *Am. J. Physiol.* **274**, H616-H626 (1998).

Peattie R. A., Schrader T., Bluth E. I. & Comstock C. E. “Development of turbulence in steady flow through models of abdominal aortic aneurysms.” *J. Ultrasound Med.* **13**, 467-472 (1994).

Peattie R.A., Asbury C. L., Bluth E. I. & Ruberti J. W. “Steady flow in models of abdominal aortic aneurysms. Part I: Investigation of the velocity patterns.” *J. Ultrasound Med.* **15**, 679-688 (1996).

- Pedersen E. M., Agerbaek M., Kristensen I. B. & Yoganathan A. P. "Wall shear stress and early atherosclerotic lesions in the abdominal aorta in young adults." *Eur. J. Vasc. Endovasc. Surg.* **13**, 443–451 (1997).
- Pedersen E., Sung H., Burlson A. & Yoganathan A. "Two-dimensional velocity measurements in a pulsatile flow model of the normal abdominal aortic simulating different hemodynamic conditions." *J. Biomech.* **26**, 1237-1247 (1993)
- Pedersen E. M., Yoganathan A. P. & Lefebvre X. P. "Pulsatile flow visualization in a model of the human abdominal aorta and aortic bifurcation." *J. Biomech.* **25**, 935–944 (1992).
- Pedley T. J. *The Fluid Mechanics of Large Blood Vessels*. Cambridge, Cambridge University Press (1979).
- Pokrovskii A. V., Dan V. N., Zlatovchen A. M. & Il'in S. A. "The impact of cardiac status and arterial hypertension on the results of surgical treatment of patients over 70 years with abdominal aortic aneurysms." *Angiol. Sosud. Khir.* **9**, 71–76 (2003).
- Prisant L. M. & Mondy J. S. "Images in hypertension: abdominal aortic aneurysms." *J. Clin. Hypertens.* **6**, 85–89 (2004).
- Purvis N. B. & Giorgio T. D. "The effects of elongational stress exposure on the activation and aggregation of blood platelets." *Biorheology.* **28**, 355–367 (1991).
- Raghavan M. L., Vorp D. A., Federle M. P., Makaroun M.S. & Webster M. W. "Wall stress distribution on three-dimensionally reconstructed models of human abdominal aortic aneurysm." *J. Vasc. Surg.* **31**, 760–769 (2001).
- Raghavan M. L. & Vorp D. A. "Toward a biomechanical tool to evaluate rupture potential of abdominal aortic aneurysm: identification of a finite strain constitutive model and evaluation of its applicability." *J. Biomech.* **33**, 475–482 (2000).
- Reilly J. M. & Tilson M. D., "Incidence and etiology of abdominal aortic aneurysms." In *Abdominal aortic aneurysms* (ed. Pierce G. E.) Philadelphia: Saunders, 689–898 (1989).
- Reininger A. J., Korndorfer M. A. & Wurzinger L. J. "Adhesion of ADP-activated platelets to intact endothelium under stagnation point flow in vitro is mediated by the integrin  $\alpha$ IIb $\beta$ 3." *Thromb. Haemost.* **79**, 998–1003 (1998).
- Reininger A. J., Reininger C. B., Heinzmann U. & Wurzinger L. J. "Residence time in niches of stagnant flow determines fibrin clot formation in an arterial branching model – detailed flow analysis and experimental results." *Thromb. Haemost.* **74**, 916-922 (1995).

- Rhoads D. N., Eskin S. G. & McIntire L. V. "Fluid flow releases fibroblast growth factor-2 from human aortic smooth muscle cells." *Arterioscler. Thromb. Vasc. Biol.* **20**, 416-421 (2000).
- Richardson E. G. & Tyler W. "The transverse velocity gradient near the mouths of pipes in which an alternating or continuous flow of air is established." *Proc. Phys. Soc. Lond.* **42**, 1-15 (1929).
- Rosenson-Schloss R. S., Vitolo J. L. & Moghe P. V. "Flow-mediated cell stress induction in adherent leukocytes is accompanied by modulation of morphology and phagocytic function." *Med. Biol. Eng. Comput.* **37**, 257-263 (1999).
- Salo J. A., Soisalon-Soininen S., Bondestam S. & Mattila P. S. "Familial occurrence of abdominal aortic aneurysm." *Ann. Intern. Med.* **130**, 637-642 (1999).
- Samy, A. K., Whyte B. & MacBain, G., "Abdominal aortic aneurysm in Scotland." *Br J. Surg.* **81**, 1104-1106 (1994).
- Satta J., Laara E. & Juvonen T. Intraluminal thrombus predicts rupture of an abdominal aortic aneurysm. *J. Vasc. Surg.* **23**, 737-739 (1996).
- Schowalter D. G., Van Atta C. W. & Lasheras J. C. "A study of streamwise vortex structure in a stratified shear layer." *J. Fluid Mech.* **281**, 247-291 (1994).
- Schrader T., Peattie R. A., Bluth E. I. & Comstock C. E. "A qualitative investigation of turbulence in flow through a model abdominal aortic aneurysm." *Invest. Radiol.* **27**, 515-519 (1992).
- Schurink G. W., van Baalen J. M., Visser M. J. & van Bockel J. H., "Thrombus within an aortic aneurysm does not reduce pressure on the aneurysmal wall." *J. Vasc. Surg.* **31**, 501-506 (2000).
- Shah P. M., Scarton H. A. & Tsapogas M. J. "Geometric anatomy of the aortic-common iliac bifurcation." *J. Anat.* **126**, 451-458 (1978).
- Shankaran H., Alexandridis P. & Neelamegham S. "Aspects of hydrodynamic shear regulating shear-induced platelet activation and self-association of von Willebrand factor in suspension." *Blood.* **101**, 2637-2645 (2003).
- Singh K., Bønaa K. H., Jacobson B. K., Bjørk L. & Solberg S. "Prevalence of and risk factors for abdominal aortic aneurysms in a population-based study." *Am. J. Epidemiol.* **154**, 236-244 (2001).
- Spagnoli L. G., Villaschi S., Neri L. & Palmieri G., "Gap junctions in myoendothelial bridges of rabbit carotid arteries." *Experientia.* **38**, 124-125 (1982).

- Stefanadis C., Tsiamis E., Vlachopoulos C., Stratos C., Toutouzas K., Pitsavos C., Marakas S., Boudoulas H. & Toutouzas P. “Unfavorable effects of smoking on the elastic properties of the human aorta.” *Circulation*. **95**, 31–384 (1997).
- Stefanadis C., Vlachopoulos C., Tsiamis E., Diamantopoulos L., Toutouzas K., Giatrakos N., Vaina S., Tsekoura D. & Toutouzas P. “Unfavorable effects of passive smoking on aortic function in men.” *Ann. Intern. Med.* **128**, 426–434 (1998).
- Sterpetti A. V., Feldhaus R. J., Schultz R. D. & Blair E. A. “Identification of abdominal aortic aneurysm patients with different clinical features and clinical outcomes.” *Am. J. Surg.* **156**, 466–469 (1988).
- Sterpetti<sup>1</sup> A. V., Cucina A., D’Angelo L. S., Cardillo B. & Cavallaro A. “Response of arterial smooth muscle cells to laminar flow.” *J. Cardiovasc. Surg. (Torino)*. **33**, 619–624 (1992).
- Sterpetti<sup>2</sup> A. V., Cucina A., Napoli F., Shafer H., Cavallaro A. & D’Angelo L. S. “Growth factor release by smooth muscle cells is dependent on haemodynamic factors.” *Eur. J. Vasc. Surg.* **6**, 636–638 (1992).
- Stringfellow M. M., Lawrence P. F. & Stringfellow R. G., “The influence of aorta-aneurysm geometry upon stress in the aneurysm wall.” *J. Surg. Res.* **42**, 425–433 (1987).
- Stroud J. S., Berger S. A. & Saloner D. “Influence of stenosis morphology on flow through severely stenotic vessels: implications for plaque rupture.” *J. Biomech.* **33**, 443–455 (2000).
- Sumner D. S., Hokanson D. E. & Strandness D. E., Jr. “Stress-strain characteristics and collagen-elastin content of abdominal aortic aneurysms.” *Surg. Gynecol. Obstet.* **130**, 459–466 (1970).
- Sutera S. P., Nowak M. D., Joist J. H., Zeffren D. J. & Bauman J. E. “A programmable, computer-controlled cone-plate viscosimeter for the application of pulsatile shear stress to platelet suspensions.” *Biorheology*. **25**, 449–459 (1988).
- Szilagy D. E. “Clinical diagnosis of intact and ruptured abdominal aortic aneurysms.” In *Aneurysms, diagnosis and treatment* (ed. Bergan J. J. & Yao J. S.). New York: Grune & Stratton. 205–215 (1982).
- Tardy Y., Resnick N., Nagel T., Gimbrone M. & Dewey C. “Shear stress gradients remodel endothelial monolayer in vitro via a cell proliferation-migration-loss cycle.” *Arterioscl. Thromb. Vasc. Biol.* **17**, 3102–3106 (1997).
- Taylor C. A., Cheng C. P., Espinosa L. A., Tang B. T., Parker D. & Herfkens R. J. “*In vivo* quantification of blood flow and wall shear stress in the human

abdominal aorta during lower limb exercise.” *Ann. Biomed. Eng.* **30**, 402–408 (2002).

Taylor L. M., Jr & Porter J. M. “Basic data related to clinical decision-making in abdominal aortic aneurysms.” *Ann. Vasc. Surg.* **1**, 502–504 (1987).

Taylor T. W. & Yamaguchi T. “Three-dimensional simulation of blood flow in an abdominal aortic aneurysm – steady and unsteady flow cases.” *J. Biomech. Eng.* **116**, 89–97 (1994).

Thompson R. W., Liao S. & Curci J. A. “Vascular smooth muscle cell apoptosis in abdominal aortic aneurysms.” *Coron. Artery Dis.* **8**, 623- (1997).

Thubrikar M. J., al-Soudi J. & Robicsek F. “Wall stress studies of abdominal aortic aneurysm in a clinical model.” *Ann. Vasc. Surg.* **15**, 355–366 (2001).

Thubrikar M. J., Labrosse M., Robicsek F., Al-Soudi J. & Fowler B., “Mechanical properties of abdominal aortic aneurysm wall.” *J. Med. Eng. Technol.* **25**, 133–142 (2001).

Thubrikar M. J., Robicsek F., Labrosse M., Chervenkov V. & Fowler B. L. “Effect of thrombus on abdominal aortic aneurysm wall dilation and stress.” *J. Cardiovasc. Surg.* **44**, 67–77 (2003).

Topper J. N., Cai J., Falb D. & Gimbrone M. A. “Identification of vascular endothelial genes differentially responsive to fluid mechanical stimuli: cyclooxygenase-2 manganese superoxide dismutase, and endothelial cell nitric oxide synthase are selectively up-regulated by steady laminar shear stress.” *Proc. Natl. Acad. Sci. USA.* **93**, 10417–10422, (1996).

Traub O. & Berk B. C. “Laminar shear stress: mechanisms by which endothelial cells transduce an atheroprotective force.” *Arterioscler. Thromb. Vasc. Biol.* **18**, 677–685 (1998).

Treska V. & Certik B. “Small aneurysms of the abdominal aorta.” *Rozhl. Chir.* **78**, 613–617 (1999).

Tsao R., Jones S. A., Giddens D. P., Zarins C. K. & Glagov S. “An automated three-dimensional particle tracking technique for the study of modeled arterial flow fields.” *J. Biomech. Eng.* **117**, 211–218 (1995).

Tzima E., Del Pozo M. A., Kiosses W. B., Mohamed S. A., Li S., Chien S. & Schwarz M. A. “Activation of Rac1 by shear stress in endothelial cells mediates both cytoskeletal reorganization and effects on gene expression.” *EMBO J.* **21**, 6791–6800 (2002).

- Viswanath N., Rodkiewicz C. M. & Zajac S. "On the abdominal aortic aneurysms: pulsatile state considerations." *Med. Eng. Phys.* **19**, 343–351 (1997).
- Vorp D. A., Wang D. H. J., Webster M. W. & Federspiel W. J. "Effect of intraluminal thrombus thickness and bulge diameter on the oxygen diffusion in abdominal aortic aneurysm." *J. Biomech. Eng.* **120**, 579–583 (1998).
- Vorp D. A., Lee P. C., Wang D. H., Makaroun M. S., Nemoto E. M., Ogawa S. & Webster M. W. "Association of intraluminal thrombus in abdominal aortic aneurysm with local hypoxia and wall weakening." *J. Vasc. Surg.* **34**, 291–299 (2001).
- Walpola P. L., Gotlieb A. I. & Langille B. L. "Monocyte adhesion and changes in endothelial cell number, morphology and F-actin distribution elicited by low shear stress in vivo." *Am. J. Pathol.* **142**, 1392–1400 (1993).
- Wang D. H., Makaroun M. S., Webster M. W. & Vorp D. A. "Mechanical properties and microstructure of intraluminal thrombus from abdominal aortic aneurysms." *J. Biomech. Eng.* **123**, 536–539 (2001).
- Wang D. H., Makaroun M. S., Webster M. W. & Vorp D. A. "Effect of intraluminal thrombus on wall stress in patient-specific models of abdominal aortic aneurysms." *J. Vasc. Surg.* **36**, 598–604 (2002).
- Wang D. M. & Tarbell J. M. "Modeling interstitial flow in an artery wall allows estimation of wall shear stress on smooth muscle cells." *J. Biomech. Eng.* **117**, 358–363 (1995).
- Warabi E., Wada Y., Kajiwara H., Kobayashi M., Koshiya N., Hisada T., Shibata M., Ando J., Tsuchiya M., Kodama T. & Noguchi N. "Effect on endothelial cell gene expression of shear stress, oxygen concentration, and low-density lipoprotein as studied by a novel flow cell culture system." *Free Radic. Biol. Med.* **37**, 682–694 (2004).
- Wilmink A. B. M., Quick C. R. G., Hubbard C. S. & Day N. E. "The association between connective tissue laxity and the risk of an abdominal aortic aneurysm." *Eur. J. Vasc. Endovasc. Surg.* **20**, 290–295 (2000).
- White J. V. & Mazzocco S. L. "Formation and growth of aortic aneurysms induced by adventitial elastolysis." In *The abdominal aortic aneurysm: genetics, pathophysiology, and molecular biology* (ed. Tilson M. D. & Boyd C. D.) New York, N. Y. New York Academy of Sciences (1996).
- Womersley J. R. "Flow in the larger arteries and its relation to the oscillating pressure." *J. Physiol.* **124**, 31–2P (1954).

- Wootton D. M., Markou C. P., Hanson S. R. & Ku D. N. "A mechanistic model of acute platelet accumulation in thrombogenic stenoses." *Ann. Biomed. Eng.* **29**, 321-329 (2001).
- Wurzinger L. J., Opitz R., Blasberg P. & Schmid-Schoenbein H. "Platelet and coagulation parameters following millisecond exposure to laminar shear stress." *Thromb. Haemost.* **54**, 381-386 (1985).
- Yin W., Alemu Y., Affeld K., Jesty J. & Bluestein D. "Flow-induced platelet activation in bileaflet and monoleaflet mechanical heart valves." *Ann. Biomed. Eng.* **32**, 1058-1066 (2004).
- Yip T. H. & Yu S. C. M. "Cyclic transition to turbulence in rigid abdominal aortic aneurysms models." *Fluid Dyn. Res.* **29**, 81-113 (2001).
- Yip T. H. & Yu S. C. M. "Oscillatory flows in straight tubes with an axisymmetric bulge." *Exp. Thermal Fluid Sc.* **26**, 947-961 (2002).
- Yoshida Y., Yamaguchi T., Caro C. G., Glagov S. & Nerem R. M. "Role of blood flow in atherogenesis." *Proceedings of the International Symposium, Hyogo*, October 1987, Springer-Verlag (1987).
- Yu S. C. M., Chan W. K., Ng B. T. H. & Chua L. P. "A numerical investigation on the steady and pulsatile flow characteristics in axi-symmetric abdominal aortic aneurysm models with some experimental evaluation." *J. Med. Eng. Tech.* **23**, 228-239 (1999).
- Yu S. C. M. "Steady and pulsatile flow characteristics in Abdominal Aortic Aneurysm models using Particle Image Velocimetry." *Int. J. Heat Fluid Flow* **21**, 74-83 (2000).
- Yu S. C. M. & Zhao J. B. "A particle image velocimetry study on the pulsatile flow characteristics in straight tubes with an asymmetric bulge." *Proc. Inst. Mech. Eng. C.* **214**, 655-671 (2002).
- Zarins C. K. & Glagov S. "Aneurysms and obstructive plaques: differing local responses to atherosclerosis." In *Aneurysms, diagnosis and treatment* (ed. Bergan J. J. & Yao J. S.) New York: Grune & Stratton, 61-82 (1982).
- Zarins C. K., Xu C. & Glagov S. "Atherosclerotic enlargement of the human abdominal aorta." *Atherosclerosis.* **155**, 157-164 (2001).
- Zarins C. K., Zatina M. A. Giddens D. P., Ku D. N. & Glagov S. "Shear stress regulation of artery lumen diameter in experimental atherogenesis." *J. Vasc. Surg.* **5**, 413-420 (1987).

- Zhang J. N., Bergeron A. L., Yu Q., Sun C., McIntire L. V., Lopez J. A. & Dong J. F. "Platelet aggregation and activation under complex patterns of shear stress." *Thromb. Haemost.* **88**, 817–821 (2002).
- Zhang J. N., Bergeron A. L., Yu Q., Sun C., McBride L., Bray P. F. & Dong J. F. "Duration of exposure to high fluid shear stress is critical in shear-induced platelet activation-aggregation." *Thromb. Haemost.* **90**, 672–678 (2003).
- Zhao Y., Chen B. P., Miao H., Yuan S., Li Y. S., Hu Y., Rocke D. M. & Chien S. "Improved significance test for DNA microarray data: temporal effects of shear stress on endothelial genes." *Physiol Genomics.* **12**, 1–11 (2002).